

SUPPLEMENTAL MATERIAL.

Supplemental methods

Animals

All experiments were performed in adherence to the National Institutes of Health *Guidelines on the Use of Laboratory Animals* and were approved by the Thomas Jefferson University Committee on Animal Care.

Enhanced green fluorescent protein (EGFP) transgenic mice (TG) mice with C57BL/6J background were purchased from The Jackson Laboratory (Stock 003291)¹. Adiponectin receptor 1 knock-out (AdipoR1 KO) mice with C57BL/6J background were purchased from Mutant Mouse Regional Resource Centers (MMRRC, Strain ID 11599). CTRP9 knock-out (KO) mice generated upon a C57BL/6 genetic background were provided by Dr. G. William Wong². Genotyping primers for the CTRP9 wild-type (WT) allele were: forward, 5'-CCCAGATGCACCCATTAAATTCG-3'; and reverse, 5'-CTCTGCACGTGGGCCTCACAGAGGG-3'. Primers for the CTRP9 null allele were: forward, 5'-CTTCTTCTAGTCCAGGTTGG-3'; and reverse, 5'-GTCTGTCCTAGCTTCCTCACTG-3'. All mice were housed in polycarbonate cages on a 12:12 hour light-dark photocycle, and had access to water ad libitum throughout the study period.

Materials

Recombinant human full length CTRP9 (fICTRP9, 00081-04-100) protein, recombinant human globular CTRP9 (gCTRP9, 00081-01-100) protein, and anti-CTRP9 antibody (for Western blot, A00081-03-100) were purchased from Aviscera Bioscience. An additional anti-CTRP9 rabbit polyclonal antibody (for co-immunoprecipitation and immunostaining) was provided by Dr. G. William Wong. U0126 (662005) and 3-morpholininosydnonimine (SIN-1, 567028) were purchased from sigma. DMEM/F12 1:1 media was from GE Healthcare Life Sciences (SH30272.02). Fetal bovine serum (FBS) was from Atlanta Biologicals (S11150). 0.25% trypsin-EDTA was purchased from Thermo Fisher Scientific (25200-056).

ADSCs isolation and expansion

ADSCs were isolated from male EGFP TG mice or littermate C57BL/6J control mice as previously reported³, with slight modification. In brief, inguinal subcutaneous adipose tissue was excised and minced in phosphate-buffered saline (PBS) on ice. The minced tissue was then digested for 1.5 hours in PBS (37°C) containing 2% bovine serum albumin (BSA) and 1 mg/ml Collagenase B (Sigma, 11088807001). The digested tissue was filtered through a 70 µm Cell Strainer (Corning, 431751) and centrifuged at 600 g for 10 minutes. After lysis of red blood cells in 1×lysis buffer containing 154mM NH₄Cl, 14mM NaHCO₃, and 0.1mM EDTA (pH = 7.3), the pellets were plated in 100 mm dishes at a density of 30,000 cells/cm² in a 1:1 mixture of Dulbecco's modified Eagle's medium (DMEM) and F12 medium containing 10% fetal bovine serum (FBS). 6 hours after the cells were plated, the medium was changed to remove nonadherent cells. The adherent cells were cultured in DMEM-F12-10% FBS and split several times to expand the cells. Cells from passage 2 (P2) were used for the experiments.

Flow cytometry

P2 ADSCs were detached from plates by trypsinization, and washed twice with PBS. For flow cytometry, 2×10⁶ ADSCs were stained at room temperature for 1 hour in staining buffer (PBS+0.5%

bovine serum albumin+2mM EDTA, pH = 7.3) with fluorescent antibodies. The following conjugated antibodies and their nonspecific negative isotype controls were employed: PE Rat Anti-Mouse CD105 (BD Biosciences, 562759), PE Rat Anti-Mouse CD31 (BD Biosciences, 551073), and their PE isotype control (BD Biosciences, 554689); FITC Rat Anti-Mouse CD90.2 (BD Biosciences, 553012) and its FITC isotype control (BD Biosciences, 553988); PE Rat Anti-Mouse CD45 (BD Biosciences, 553081), and its PE isotype control (BD Biosciences, 553989). After incubation, cells were washed 3 times with staining buffer, and centrifuged at 300×g for 5 minutes. Supernatants were aspirated and discarded. Stained cells were resuspended in PBS for flow cytometry. Surface marker expression was evaluated via flow cytometry (BD LSRFortessa). Data analysis was performed with BD CellQuest software at the Sidney Kimmel Cancer Center at Thomas Jefferson University.

Adipogenesis and Osteogenesis

Adipogenic and osteogenic differentiation of ADSCs were performed as previously reported⁴. ADSCs (Passage 2) were plated at a density of 2.5×10^4 cells/cm² in growth medium for 16 hours to allow attachment.

For adipogenesis, cells were incubated for 21 days in adipogenic medium [low-glucose DMEM supplemented with 10% FBS, 2 mM L-glutamine, 100 U/ml penicillin, 100 µg/ml streptomycin (Thermo Fisher Scientific, 15140122), 100 µM L-ascorbate acid (Sigma, A5960), 1 µM dexamethasone (Sigma, D1756), 0.5 mM 1-methyl-3-isobutylxanthine (Sigma, I5879), 100 µM indomethacin (Sigma, I7378), and 10 µg/ml human recombinant insulin (Sigma, 91077C)]. Control group cells were cultured in low-glucose DMEM plus 10% FBS (control medium). The medium was changed every 3 days. Adipogenesis was assessed by incubating cells with Oil Red O solution (Sigma, O0625) to stain cytoplasmic neutral lipids.

For osteogenesis, cells were incubated in 24-well plates at 100% confluence with osteogenic medium [high-glucose DMEM supplemented with 10% FBS, 100 nM dexamethasone (Sigma, D4902), 10 mM β-glycerol phosphate (Sigma, 50022), and 200 µM L-ascorbic acid]. The medium was changed every 3 days. Control group cells were cultured in high-glucose DMEM plus 10% FBS. Differentiation was visualized via phase-contrast microscope after 21 days, by Alizarin-Red Staining Solution (Sigma, TMS-008).

Animal study protocol

Permanent myocardial infarction (MI) surgery was performed by ligating the left anterior descending coronary artery⁵. Immediately after MI, 1×10^5 ADSCs suspended in 25µL PBS (containing 0.2mM EDTA, pH=7.3) were injected intramyocardially into the infarct border zone in three different sites. MI control animals received saline injection only and sham control animals were subjected to all surgical procedures except for ligation of the coronary artery and intramyocardial injection.

For long-term observations (including echocardiographic, hemodynamic, and survival studies), a total of 166 adult male C57BL/6J mice were randomly subjected to the following groups: (1) Sham (n=12); (2) MI+vehicle (n=45); (3) MI+gCTRP9 (0.25 µg/g/d via peritoneal implant osmotic pumps for 2 weeks, n=30); (4) MI+ADSC+vehicle (1×10^5 Passage 2 cells directly injected into peri-infarct area immediately post-MI, n=42); or (5) MI+ADSC+gCTRP9 (n=37).

For histological analysis (including GFP immunostaining and TUNEL staining), 100 adult male C57BL/6J mice were randomly subjected to the following groups: (1) Sham (n=4); (2) MI+vehicle (n=6); (3) MI+gCTRP9 (n=6); (4) MI+ADSC+vehicle (n=30); (5) MI+ADSC+gCTRP9 (n=30); (6)

MI+scN-cad-ADSC+gCTRP9 (n=12); or (7) MI+siN-cad-ADSC+gCTRP9 (n=12). Additionally, 30 adult male CTRP9 KO mice were subjected to MI+ADSC+vehicle.

Echocardiography

M-mode images of mice subjected to 1-2% isoflurane anesthesia were obtained via Visualsonics 770 echocardiography machine (Canada), as previously described ⁵. Hearts were viewed in the short-axis between the two papillary muscles. Each measurement was obtained with M-mode by averaging results from three consecutive heart beats. LV internal dimensions (LVID) at diastole and systole (LVIDd and LVIDs) were measured. LV ejection fraction (EF) was automatically calculated by the echocardiography software using the formulas: $EF(\%)=100 \times [(LVIDd^3 - LVIDs^3) / LVIDd^3]$.

Hemodynamic study

In vivo cardiac hemodynamic function was evaluated 12 hours or 4 weeks after MI utilizing a Millar tip-pressure catheter, as previously described ⁵. Mice were anesthetized with 1-2% isoflurane. The right common carotid artery was isolated and cannulated (1.4 French micromanometer, Millar Instruments). LV pressure, LV end-diastolic pressure (LVEDP), and heart rate (HR) were measured by catheter advancement into the LV cavity. Data was recorded and analyzed on a PowerLab System (USA). These parameters, as well as maximal values of the instantaneous first derivative of LV pressure (+dP/dt_{max}, a measure of cardiac contractility), and minimum values of the instantaneous first derivative of LV pressure (-dP/dt_{min}, a measure of cardiac relaxation), were recorded.

Masson's trichrome staining

Masson's trichrome staining evaluated cardiac interstitial fibrosis and structural changes ⁶. Five sections (5 μm thick) per heart were prepared for masson's trichrome staining per manufacturer's instructions (Sigma, HT15). Fibrosis was measured via Olympus cellSens Microscope Imaging Software, and determined by fibrosis area/LV area.

Neonatal mouse ventricular cardiomyocytes isolation

Primary cultures of neonatal mouse ventricular myocytes (NMVMs) from 1-2 day-old C57BL/6 mouse pups were prepared via previously described method ⁷, slightly modified. Immediately after euthanasia of mouse pups, hearts were removed, ventricles were minced, and myocytes were isolated with 1.0 mg/mL collagenase type II (ThermoFisher scientific, 17101015). Isolated myocytes were collected at 10 minute intervals until complete tissue digestion. Cells were re-suspended in high glucose DMEM (Sigma, D5796) containing 10% FBS, 10mM HEPES, and 0.1 mM 5-Bromo-2'-deoxyuridine (BrdU, Sigma, B5002), and plated in culture dishes for 90 minutes to allow attachment of fast-adherent fibroblasts. Non-adherent cells (ventricular myocytes) were collected and plated in 6-well plates coated with Applied Cell Extracellular Matrix (abm, G422; for co-culture with ADSCs and caspase-3 activity) or Millicell EZ SLIDE 8 well glass (Sigma, PEZGS0816; for TUNEL assay). On the following day, the medium was replaced with M199 containing 0.5% FBS, 10mM HEPES, and no BrdU.

Co-culture of ADSCs with cardiomyocytes

ADSCs and NMVMs were co-cultured at 1:10 ratio in 6-well plates separated by Corning cell culture inserts (Sigma, CLS3414), as previously described ⁸. The semi-permeable membranes (pore size 3.0

µm) within these inserts allow cellular-secreted factor diffusion, but prevent cellular migration or transport. Neonatal cardiomyocytes and ADSCs were respectively plated in the lower and upper insert. The co-culture system was then treated with gCTRP9 (2.0µg/mL) or vehicle for 7 days. ADSCs co-cultured with ADSCs served as a control group. Sodium butyrate (Sigma, B5887) was used as a positive control for inducing cardiogenic differentiation of ADSCs ⁹.

Immunohistochemistry

For *in vitro* staining, cells were fixed with 4% paraformaldehyde and were permeabilized in PBS supplemented by 0.1% Triton (Sigma, X-100) for 10 minutes ¹⁰. Cells were blocked with 1% BSA in PBS for 2 hours, and incubated overnight with primary antibody (4°C). For fixed tissues, wax blocks were cut into 5 µm thick sections, and mounted on glass slides for staining. Slides were deparaffinized, and subjected to antigen retrieval in hot citric acid buffer. After cooling, slides were permeabilized with 0.2% Triton-100 for 15 minutes and were blocked with 1% BSA in PBS for 2 hours, and incubated overnight with primary antibody (4°C). Primary antibodies were visualized with donkey anti-rabbit IgG (H+L) secondary antibody conjugated with Alexa Fluor 488 (ThermoFisher scientific, A-21206), donkey anti-rabbit IgG (H+L) secondary antibody conjugated with Rhodamine (ThermoFisher scientific, 31685), donkey anti-goat IgG secondary antibody conjugated with Texas Red (ThermoFisher scientific, PA1-28662), or goat anti-mouse IgG (H+L) secondary antibody conjugated with Rhodamine RedTM-X (Jackson immunoresearch, 115-295-003). Nuclei in both cells and embedded tissues were stained with 4',6-diamidino-2-phenylindole (DAPI, Vector Laboratories, H-1200). Micrographs of all immunostains were acquired via Olympus BX51 Fluorescence Microscope (Japan) and Olympus DP72 camera (Japan).

The primary antibodies used in this study included: anti-N-cadherin mouse monoclonal antibody (ab98952) (1/200), anti-CTRP9 rabbit polyclonal antibody (a gift from Dr. G. William Wong) (1/100), anti-CD45 goat polyclonal antibody (R&D Systems, AF114), anti-Nrf2 rat monoclonal antibody (CST, #14596) (1/100), anti-GFP rabbit polyclonal antibody (Genescript, A01704) (1/200), and anti-Troponin T mouse monoclonal antibody (ThermoFisher scientific, MS-295-P0) (1/1,000).

Leukocyte accumulation

Effect of gCTRP9, ADSCs or their combination upon leukocyte accumulation in peri-infarct region was determined by CD45 immunostaining as previously reported ^{6, 11, 12} 7 days after MI, when the total number of leukocytes reached a maximum level ¹³. Briefly, cardiac tissue was fixed and slides were prepared as described above. Immunofluorescent staining was performed with primary antibody (anti-CD45 goat polyclonal antibody) followed by donkey anti-goat IgG secondary antibody conjugated with Texas Red to identify infiltrated leukocytes. Slides were counter-stained with DAPI (blue) and visualized with an Olympus BX51 Fluorescence Microscope (40X). Images were captured with Olympus DP72 camera and number of red stained cells was quantified by Olympus Image Analysis software. Leukocytes infiltration was expressed as CD45+ leukocytes/mm².

Quantitative PCR

RNA was extracted from cells via RNeasy Mini Kit (Qiagen, 74106), per manufacturer's instructions. cDNA was prepared from 1 µg total RNA using SuperScript III First-Strand Synthesis System (ThermoFisher scientific, 18080051), per manufacturer's protocol. PCR was performed via 7900HT Fast Real-Time PCR System (Applied Biosystems) at the Sidney Kimmel Cancer Center at Thomas

Jefferson University. Samples were analyzed in triplicate 10 μ l reactions, per SYBR Green PCR Master Mix protocol (ThermoFisher scientific, 4472908). Primers were purchased from Integrated DNA Technologies (listed in Supplemental Table 1). GAPDH and β -actin served as housekeeping targets. Data were normalized via standard comparative CT method. Expression patterns were visualized as heat maps using Heml Heatmap Illustrator ¹⁴.

Cell growth assay

P2 ADSCs were plated at 3,000 cells/well in 96-well plates. Cell population viability was determined over time via Cell Counting Kit-8 (CCK-8) (Sigma, 96992), per manufacturer protocol. The absorbance at 450 nm was read using the SpectraMax M5 microplate reader (Molecular Devices).

Wound healing assay

Cells were seeded into the Culture-Insert 2 Well of 35 mm μ -Dish (Ibidi, 81176). After treatments, cells were starved with serum-free medium overnight. The culture insert was removed before a ~ 500 μ m cell-free gap was created. The dish was then overlaid with culture medium. Cellular migration was visualized at the indicated time. Wound-healing percentage of the cells was determined by the ratio of: healing width at each time point to wound width at time 0.

Transwell study and violet staining

Modified two-chamber plates, pore size 8 μ m, were employed (Sigma, CLS3464). 2 \times 10⁴ ADSCs were seeded in serum-free medium in the upper chamber. ADSCs were added to the top chamber coated with matrigel (Corning, 354248). To stimulate migration, complete medium was added to the bottom wells. After 24 hours incubation (37°C), cells in the upper chamber were carefully removed with a cotton swab. Cells that had traversed the membrane were stained with 0.1% Crystal Violet (Sigma, C0775), and counted via microscopy (Olympus BX51).

Western blot analysis

Total proteins were isolated from cells or heart tissues with 1 \times lysis buffer (CST #9803: 20 mM Tris-HCl pH 7.5, 150 mM NaCl, 1 mM Na₂EDTA, 1 mM EGTA, 1% Triton, 2.5 mM sodium pyrophosphate, 1 mM β -glycerophosphate, 1 mM Na₃VO₄, and 1 μ g/ml leupeptin) supplemented by a protease inhibitor cocktail (Thermo Fisher Scientific, 78438). Nuclear and cytoplasmic proteins were prepared by a Nuclear and Cytoplasmic Extraction Kit (Thermo Fisher Scientific, 78833), as described previously ¹⁵. 30-70 μ g of protein per sample was separated via gel electrophoresis, transferred to a poly-vinylidene fluoride membrane, and blocked with 5% milk for 1 hour. The membrane was incubated overnight with primary antibodies (4°C). The membranes were then incubated with secondary HRP-conjugated anti-mouse antibody (CST #7076, 1/10,000) or anti-rabbit antibody (CST #7074, 1/10,000) at room temperature for 2 hours, and exposed to enhanced chemiluminescent (ECL) substrate (Thermo Fisher Scientific, 34096). Western blot results were quantified by densitometry (Image Lab).

The primary antibodies used in this study were: anti-cleaved caspase-3 rabbit polyclonal antibody (CST #9661) (1/1,000), anti-caspase-3 rabbit polyclonal antibody (CST #9662) (1/1,000), anti-MMP-3 mouse monoclonal antibody (SC-21732) (1/1,000), anti-MMP-9 rabbit polyclonal antibody (ab38898) (1/1,000), anti-Metallothionein rabbit polyclonal antibody (ab36882) (1/1,000), anti-Sod-2 rabbit monoclonal antibody (CST #13141) (1/1,000), anti-Sod-3 rabbit polyclonal antibody

(LSBio, LS-C407959) (1/1,000), anti-HO-1 rabbit polyclonal antibody (CST #7008) (1/1,000), anti-Prdx1 rabbit monoclonal antibody (CST #8499) (1/1,000), anti-phospho-Akt rabbit polyclonal antibody (CST #9271) (1/1,000), anti-Akt rabbit monoclonal antibody (CST #4691) (1/1,000), anti-phospho-AMPK α rabbit polyclonal antibody (CST #2531) (1/1,000), anti-AMPK α rabbit monoclonal antibody (CST #2603) (1/1,000), anti-phospho-ERK1/2 mouse monoclonal antibody (CST #9106) (1/1,000), anti-ERK1/2 mouse monoclonal antibody (CST #9107) (1/1,000), anti-N-cadherin rabbit polyclonal antibody (LSBio, LS-B12904) (1/1,000), anti-N-cadherin mouse monoclonal antibody (ab98952) (1/1,000), anti-Nrf2 rabbit monoclonal antibody (CST #1272) (1/1,000), anti-H3 rabbit polyclonal antibody (Millipore, 06-599) (1/1,000), anti- β -tubulin rabbit monoclonal antibody (CST #2128) (1/1,000), anti- β -actin mouse monoclonal antibody (sc-47778), and anti-GAPDH rabbit monoclonal antibody (CST #2118) (1/1,000).

In-gel zymography

In-gel zymography was performed to assess the relative gelatinase (MMP-2 and MMP-9) content and has been described in detail previously¹⁶. Briefly, protein samples (50 μ g/sample) and conditioned medium (1 μ g/per sample) of ADSCs were mixed with 5 \times non-reducing loading buffer (H₂O supplemented with 4% SDS, 20% glycerol, and 0.01% bromophenol blue, 125mM Tris-HCl). Next, they were subjected to electrophoretic separation over a substrate containing gelatin (1 mg/mL type A gelatin, Sigma, G1890). After electrophoresis, the gels were twice washed in wash solution (H₂O supplemented with 2.5% Triton X-100, 50 mM Tris-HCl, 5 mM CaCl₂, 1 μ M ZnCl₂, Ph=7.5) for 30 minutes each at room temperature, followed by incubation solution (H₂O supplemented with 1% Triton X-100, 50 mM Tris-HCl, 5 mM CaCl₂, 1 μ M ZnCl₂, Ph=7.5) for 24 hours at 37°C. The gels were immersed in staining solution (H₂O containing 0.5% coomassie blue, 40% v/v methanol and 10% v/v acetic acid) for 60 minutes, and washed in destaining solution (H₂O containing 40% v/v methanol and 10% v/v acetic acid) until bands were clearly seen. The gels were stored in 5% acetic acid. Gelatinolytic signals were analyzed via densitometric methods (ChemiDoc MP imaging system, BioRad).

Determination of apoptosis

Apoptosis of ADSCs, cardiomyocytes, and myocardium were determined by terminal deoxynucleotidyl transferase-mediated dUTP nick-end labeling (TUNEL) staining and caspase-3 activity, as described previously¹⁷. TUNEL staining was performed via Roche In Situ Cell Death Detection Kit (Sigma, 11767305001 and 11767291910) per manufacturer's protocol. The index of apoptosis was determined by number of TUNEL positive nuclei/the total nuclei. Caspase-3 activity assay was performed by ApoAlert Caspase-3 Colorimetric Assay kit (Takara, 630217), per manufacturer protocol.

LDH assay

LDH release assay determined oxidative stress-induced cell death¹⁸. We employed the LDH Cytotoxicity Detection kit (Takara, MK401), and following manufacturer protocol. After treatment, cells were exposed to the indicated concentration of H₂O₂ for 3 hours. The cell medium was then collected and centrifuged at 250 \times g for 10 minutes. 100 μ l of the supernatant was mixed with an equal volume of pre-prepared solution (catalyst/dye buffer ratio = 1:45) for 30 minutes at room temperature in a 96-well plate. The absorbance of samples at 490 nm was measured via SpectraMax

M5 microplate reader (Molecular Devices). The percentage of LDH release in each sample was compared to the absorbance value from cells pretreated with 0.5% Triton X-100.

Conditioned medium collection and preparation

We employed a modified method to prepare the conditioned medium (CM) of ADSCs⁷. CM was generated as follows: Passage 2 ADSCs were grown to 90% confluence in 6-well dishes, and incubated for 24 hours with gCTRP9 (2.0µg/mL) or vehicle. The culture medium was washed and replaced by serum-free DMEM/F12 medium. After another 24 hours, CM was collected, and 1) used for cardiomyocyte treatment, or 2) stored at -80°C for future use. The protein concentration of CM was determined by Bio-Rad Protein Assay (# 500-0006). For protein analysis, 250µL CM (about 10µg protein) per sample was concentrated by heat evaporation to 30µL and loaded for electrophoresis. After electrophoresis, the gel was subjected to colloidal blue staining, per manufacturer protocol (Thermo Fisher Scientific, LC6025).

Production and purification of recombinant flag-flCTRP9

Mammalian expression vector (pCDNA3.1) encoding C-terminal flag-tagged flCTRP9 construct was provided by Dr. G. William Wong¹⁹. For cell transfection, Adeno-X-293 cells (Takara, 632271) were cultured in DMEM containing 10% fetal bovine serum (FBS) supplemented with 2 mM L-glutamine, 100 U/ml penicillin, and 100 µg/ml streptomycin. Transient transfections were performed in Adeno-X-293 cells using Lipofectamine 3000 transfection kit (Invitrogen, L3000-008) per manufacturer's protocol. 24 hours after transfection, cells were washed and cultured in serum free DMEM medium supplemented with vitamin C (0.1 mg/ml) for another 24-48 hours before the conditioned medium was collected for Western blot analysis using anti-flag M2 (Sigma, F1804) antibody. For production and purification of recombinant flag-flCTRP9, the conditioned medium was collected 3 times (every 48 hours), pooled, and purified using anti-flag M2 affinity gel (Sigma, A2220) per manufacturer's instructions (Sigma), and eluted with 150 µg/ml 3×flag peptide (Sigma, F4799). Purified proteins were dialyzed against 20 mM HEPES buffer (pH 8.0) containing 135 mM NaCl in a 10-kDa cutoff Slide-A-Lyzer dialysis cassette (Thermo Fisher Scientific, 66830).

Co-immunoprecipitation

P2 ADSCs were treated with 2µg/mL his-gCTRP9, 5µg/mL his-flCTRP9, 5 µg/ml flag-flCTRP9, or vehicle for 10 minutes. 1 mg/mL DTBP (Thermo Fisher Scientific, 20665) was added for 30 additional minutes. Cells were washed once with PBS, and lysed with cold 1×lysis buffer (CST #9803) supplemented with a protease inhibitor cocktail (Thermo Fisher Scientific, 78438). Cell lysates were then incubated with either anti-CTRP9 antibody (a gift from Dr. G. William Wong) or anti-flag M2 (Sigma, F1804) antibody, and supplemented with either protein A plus ultralink resin (Thermo Fisher Scientific, 53142) or protein G plus ultralink resin (Thermo Fisher Scientific, 53128) and rocked overnight (4°C). For in tube assay, 2µg human recombinant CTRP9 (Novus, H00338872-P01), 2µg human recombinant N-cadherin (LSBio, LS-G27859), and 1 mg/mL DTBP (Thermo Fisher Scientific, 20665) were mixed in 500µl cold 1×lysis buffer (CST #9803). This mixture was then incubated with anti-CTRP9 antibody and protein A plus ultralink resin (Thermo Fisher Scientific, 53142) and rocked overnight (4°C).

The protein A beads were washed extensively with lysis buffer. Proteins were eluted from the beads and resolved by IgG elution buffer (Thermo Fisher Scientific, 1856202). Samples containing reducing

agent (dithiothreitol) were heated and separated by electrophoresis. After transfer to polyvinylidene fluoride membranes, proteins were immunoblotted with anti-N-cadherin mouse monoclonal antibody (ab98952) (1/1,000) as described above.

Small interfering RNA (siRNA)-mediated gene knockdown

N-cadherin siRNA duplex and its scrambled RNA²⁰ were synthesized by Integrated DNA Technologies. Nrf2 siRNA and its scramble RNA were purchased from Qiagen. When ADSCs reached 80% confluence, cells were transfected with siRNA via HiPerFect Transfection Reagent (Qiagen, 301705) per manufacturer protocol (final siRNA concentration: 100 nM). After 8 hours incubation (37°C), the transfection reagent-siRNA mixture was replaced with fresh growth medium. 72 hours after transfection, the cells were harvested for further experiments.

Silver staining and mass spectrometric sample Preparation

After separation by electrophoresis, the co-immunoprecipitated proteins were visualized by silver staining as previously described²¹. Briefly, the gels were fixed in 12% Trichloroacetic acid (TCA, Sigma, T6399) solution for 30 minutes, and rinsed twice by deionized water. The gels were twice immersed in a fixative solution (containing 40% v/v methanol and 10% v/v acetic acid) for 30 minutes each followed by wash solution (containing 10% v/v ethanol and 5% v/v acetic acid) twice for 30 minutes each. The gels were immersed in ferricyanide solution (containing 10g/L potassium ferricyanide and 16g/L sodium thiosulfate) for 10 minutes, and washed in deionized water until all yellow color disappeared. The gels were then twice immersed in silver nitrate solution (2g/L) for 15 minutes each and deionized water-rinsed. After incubation in the development solution (sodium carbonate, 30 g/L; 37% formaldehyde, 0.25 mL/L; sodium thiosulfate, 10 mg/L) for 5-10 minutes until sufficiently developed, the reaction was terminated by 5% acetic acid.

For mass spectrometric analysis, the corresponding silver-stained gel spots were excised and sent to the Proteomics and Metabolomics Facility at the Wistar Institute (University of Pennsylvania, Philadelphia).

LC-MS/MS Analyses and data Processing

Liquid chromatography tandem mass spectrometry (LC-MS/MS) analysis was performed by the Proteomics and Metabolomics Facility at the Wistar Institute by Q Exactive HF mass spectrometer (ThermoFisher Scientific) coupled with a Nano-ACQUITY UPLC system (Waters). Samples were digested in-gel with AspN and injected onto a UPLC Symmetry trap column (180 µm i.d. x 2 cm packed with 5 µm C18 resin; Waters). Tryptic peptides were separated by reversed phase HPLC on a BEH C18 nanocapillary analytical column (75 µm i.d. x 25 cm, 1.7 µm particle size; Waters) using a 95 min gradient formed by solvent A (0.1% formic acid in water) and solvent B (0.1% formic acid in acetonitrile). A 30 minute blank gradient was run between sample injections to minimize carryover. Eluted peptides were analyzed by the mass spectrometer set to repetitively scan m/z from 300-2000 in positive ion mode. The full MS scan was collected at 60,000 resolution followed by data-dependent MS/MS scans at 15,000 resolution on the 20 most abundant ions exceeding a minimum threshold of 20,000. Peptide match was set as preferred, exclude isotopes option, and charge-state screening were enabled to reject unassigned charged ions.

Peptide sequences were identified by MaxQuant 1.5.2.8 (Ref: PMID 19029910). MS/MS spectra were searched against a UniProt mouse database (www.uniprot.org). False discovery rates for protein and

peptide identifications were set at 1%.

GFP DNA determination by quantitative PCR

The number of cells engrafted to the heart 1, 3, 7, and 14 days after transplantation was determined via quantitative PCR assessments of GFP DNA levels as previously reported^{22, 23}, with slight modification. Genomic DNA was prepared from EGFP-ADSCs and normal heart tissues via Genomic DNA Extraction Kit (Qiagen, 69506). The exogenous GFP gene was amplified for calculating the number of EGFP-ADSCs. Total mouse heart tissue genomic DNA was identified by GAPDH. 300ng purified DNA was amplified in triplicate 20 μ l reactions via SYBR Green PCR Master Mix (ThermoFisher scientific, 4472908). Amplification was performed with GFP forward (5'-ATTGCTTCAGCCGCTACCC-3'), GFP reverse (5'-AGTTCACCTTGATGCCGTTCTT-3'), GAPDH forward (5'-ATTCAACGGCACATGCAA-3'), GAPDH reverse (5'-TTCAGACTCAGTTCTTGGTTTT-3') primers. The PCR procedure is as follows: 50°C for 2 minutes, 1 cycle; 95°C for 15 minutes, 1 cycle; 95°C for 15 seconds, 53°C for 15 seconds, 72°C for 30 seconds, 40 cycles. After amplification, DNA melting curves were generated by denaturing at 95°C for 15 seconds, cooling to 60°C for 1 minute, and then increasing the temperature 0.5°C/s until reaching 95°C, while continuously monitoring fluorescence. Standard curves of GFP and GAPDH genes generated (by diluting the genomic DNA of EGFP-ADSCs in normal heart tissue genomic DNA at a ratio from 1:1 to 1:1,000) were used as a reference for unknown DNA samples. Cell engraftment was quantified as the number of GFP-positive cells per 100 heart cells in apex region.

CTRP9 determination by Enzyme-Linked Immunosorbent Assay (ELISA)

Plasma was collected 1 day after MI. Heart tissue in the infarct border zone was collected 1 day after MI. Protein samples were extracted from heart tissues. Total protein concentration was determined by Bio-Rad Protein Assay (# 500-0006). To each well of a 96-well plate, 50 μ L plasma or 50 μ L protein sample (~300 μ g) was loaded. Samples were analyzed in triplicate via mouse CTRP9 ELISA kit (Aviscera Bioscience, SK00081-08).

Online Table 1. Real Time PCR Primers

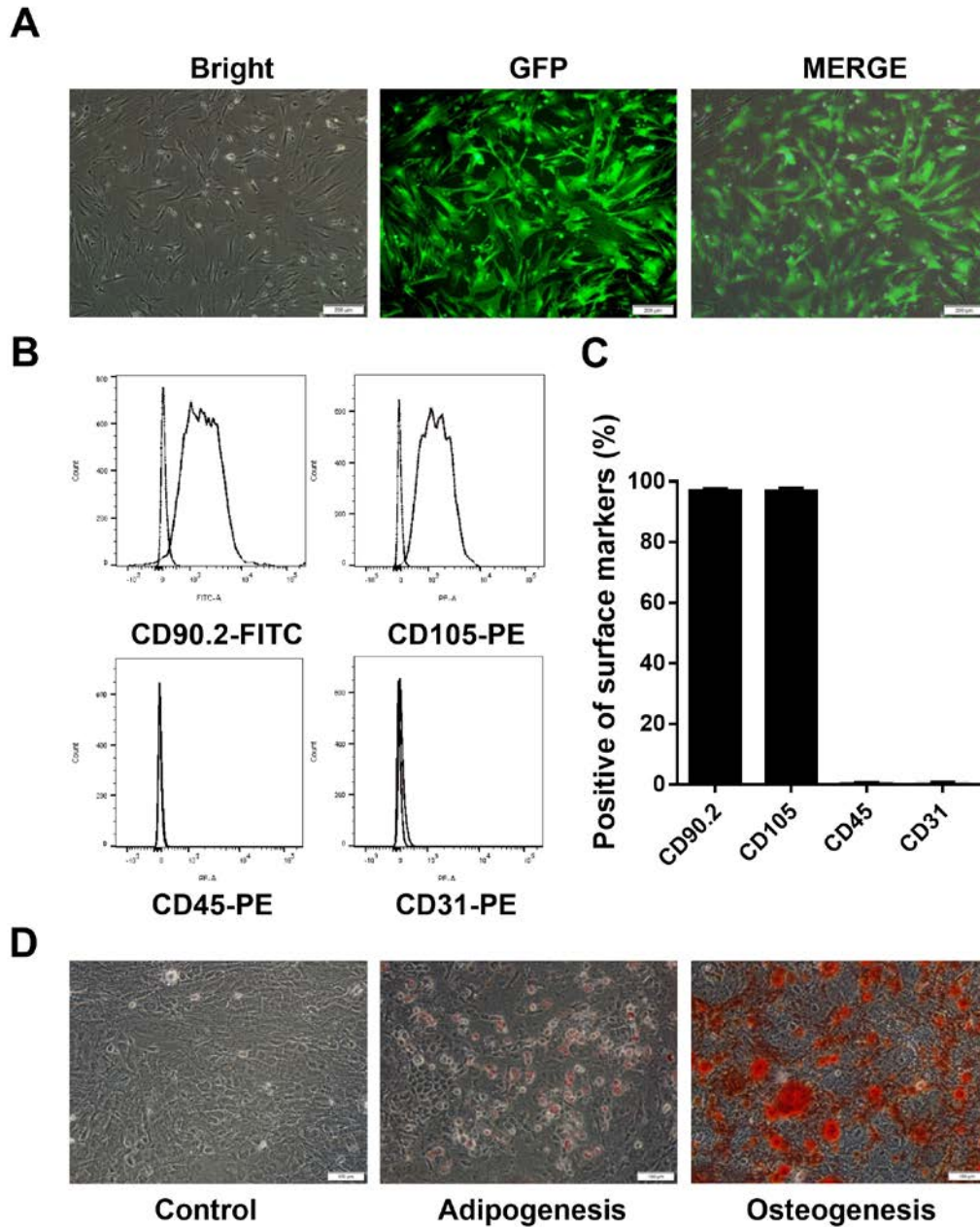
Gene profile	Genes	Forward primer (5'–3')	Reverse primer (5'–3')
Housekeeper	Gapdh	AGGTCGGTGTGAACGGATTTG	TGTAGACCATGTAGTTGAGGTCA
	Actb (β -actin)	GGCTGTATTCCCCTCCATCG	CCAGTTGGTAACAATGCCATGT
Cell proliferation	Cena2	GCCTTCACCATTTCATGTGGAT	TTGCTGCGGGTAAAGAGACAG
	Ccnb1	AAGGTGCCTGTGTGTGAACC	GTCAGCCCCATCATCTGCG
	Cend1	GCGTACCCTGACACCAATCTC	CTCCTTTCGCACTTCTGCTC
	Ccne1	GTGGCTCCGACCTTTCAGTC	CACAGTCTTGTC AATCTTGGCA
	Cdkn2a (p16)	CGCAGGTTCTTGGTCACTGT	TGTTACGAAAAGCCAGAGCG
	Cdkn1a (p21)	CCTGGTGATGTCCGACCTG	CCATGAGCGCATCGCAATC
	Trp53 (p53)	GCGTAAACGCTTCGAGATGTT	TTTTTATGGCGGGAAGTAGACTG
	Pak3	TTGGATAACGAAGAAAACCCCC	GAGTCTCGGTTGTTACTGTTCAT
	Racgap1	CGCCGGATGGAGATTATCAATG	CCCCGTCTCTGCTTTC ACAA
	Nusap1	CGTCACCAAAACGAGGAGGAG	AGAAAACCTCATCCGTGCATAGAG
	Myh10	GGAATCCTTTGGAAATGCGAAGA	GCCCCAACAATATAGCCAGTTAC
	Cks2	TCGATGAGCACTACGAGTACC	CCATCTAGACTCTGTTGGACAC
	Migration	Mmp2	CAAGTCCCGGCGATGTC
Mmp3		ACATGGAGACTTTGTCCCTTTTG	TTGGCTGAGTGGTAGAGTCCC
Mmp9		GCAGAGGCATACTGTACCG	TGATGTTATGATGGTCCC ACTTG
Mmp12		GAGTCCAGCCACCAACATTAC	GCGAAGTGGGTCAAAGACAG
Mmp19		CTGTGGCTGGCATTCTTACTT	GGGCAGTCCAGATGCTTCC
Cell death	Bcl2	GTCGCTACCCTCGTGACTTC	CAGACATGCACCTACCCAGC
	Bcl2l1	GACAAGGAGATGCAGGTATTGG	TCCCGTAGAGATCCACAAAAGT
	Dapk1	ATGACTGTGTTCAGGCAGGAA	CCGGTACTTTTCTCACGACATT
	Stk17b	ATGTCTCGGAGGAGATTTCGATT	TTTTCAGGGATTGGCAGCAT
	Becn1	ATGGAGGGGTCTAAGGCGTC	TCCTCTCCTGAGTTAGCCTCT
	Map1lc3a (LC3)	TTATAGAGCGATACAAGGGGGAG	CGCCGTCTGATTATCTTGATGAG
	Sqstm1 (p62)	ATGTGGAACATGGAGGGAAGA	GGAGTTCACCTGTAGATGGGT
Paracrine function	Kitl (SCF)	CGGGATGGATGTTTTGCCTA	CTTCGGTGC GTTTTCTTCCA
	Cxcl12 (Sdf1)	TGCATCAGTGACGGTAAACCA	CACAGTTGGAGTGTGAGGAT
	Fgf2	GCTGCTGGCTTCTAAGTGTG	TACTGCCCAGTTCGTTTCAG
	Hgf	ATGTGGGGGACCAA ACTTCTG	GGATGGCGACATGAAGCAG
	Igf1	CTGGACCAGAGACCCTTTGC	GGACGGGGACTTCTGAGTCTT
Angiogenesis	Pdgfra	AGGTATGTATCCACACATGCGT	AGTTCCTGTGGTTTCATCTCG
	Pdgfrb	TTCCAGGAGTGATACCAGCTT	AGGGGGCGTGATGACTAGG
	Angpt1	CACATAGGGTGCAGCAACCA	CGTCGTGTTCTGGAAGAATGA

	Angptl2	AGCCTGAGAATACCAACCGC	CCCTTGCTTATAGGTCTCCCAG
	Vegfa	GCACATAGAGAGAATGAGCTTCC	CTCCGCTCTGAACAAGGCT
	Tgfb2	TCGACATGGATCAGTTTATGCG	CCCTGGTACTGTTGTAGATGGA
Anti-oxidation	Mt1	AAGAGTGAGTTGGGACACCTT	CGAGACAATAACAATGGCCTCC
	Mt2	GCCTGCAAAATGCAACAATGC	AGCTGCACTGTGCGGAAGC
	Mt3	ACCTGCCCTGTCTACTG	CCTTGGCACACTTCTCACATC
	Sod1	AACCAGTTGTGTTGTCAGGAC	CCACCATGTTTCTTAGAGTGAGG
	Sod2	CAGACCTGCCTTACGACTATGG	CTCGGTGGCGTTGAGATTGTT
	Sod3	CCTTCTTGTCTACGGCTTGC	TCGCCTATCTTCTCAACCAGG
	Nrf1	AGCACGGAGTGACCCAAAC	TGTACGTGGCTACATGGACCT
	Nfe2l2	TCTTGAGTAAGTCGAGAAGTGT	GTTGAAACTGAGCGAAAAAGGC
	Txn2	TGGGCTTCCCTCACCTCTAAG	CCTGGACGTTAAAGGTCGTCA
	Hmox1	AAGCCGAGAATGCTGAGTTCA	GCCGTGTAGATATGGTACAAGGA
	Nqo1	AGGATGGGAGGTACTCGAATC	AGGCGTCTTCTTATATGCTA
	Gpx1	AATGTCGCGTCTCTGAGG	TCCGAAGTATTGCACGGG
	Gpx4	GATGGAGCCCATTCTGAACC	CCCTGTACTTATCCAGGCAGA
	Prdx1	AATGCAAAAATGGGTATCCTGC	CGTGGGACACACAAAAGTAAAGT
Mitochondrial function	Ndufb5	CAAGAGACTGTTTGTGTCGAAGC	TGTTACCAGTGTTATGCCAAT
	Sdha	GGAACACTCCAAAAACAGACCT	CCACCCTGGGTATTGAGTAGAA
	Uqcrc2	AAAGTTGCCCGAAGGTTAAA	GAGCATAGTTTTCCAGAGAAGCA
	Cox6a1	TCAACGTGTTCTCAAGTCGC	AGGGTATGGTTACCGTCTCCC
	Atp5b	GGTTCATCCTGCCAGAGACTA	AATCCCTCATCGAACTGGACG
	Mdh2	TTGGGCAACCCCTTCACTC	GCCTTTCACATTGCTCTGGTC
	Idh2	GGAGAAGCCGGTAGTGGAGAT	GGTCTGGTCACGGTTTGAA
Pluripotency	Pou5f1 (OCT4)	GGCTTCAGACTTCGCCTCC	AACCTGAGGTCCACAGTATGC
	Nanog	TCTTCTGGTCCCACAGTTT	GCAAGAATAGTTCTCGGGATGAA
Cardiogenic differentiation	Nkx2-5	TGACCCAGCCAAAGACCCT	CCATCCGTCTCGGCTTTGT
	Kit (c-KIT)	CTCCCCAACAGTGTATTAC	TAGCCCGAAATCGCAAATCTT
	Nppa	GCTTCCAGGCCATATTGGAG	GGGGGCATGACCTCATCTT
	Gata4	CCCTACCCAGCCTACATGG	ACATATCGAGATTGGGGTGTCT
Endothelial differentiation	Pecam1 (CD31)	CTGCCAGTCCGAAAATGGAAC	CTTCATCCACCGGGGCTATC
	Kdr (Flk-1)	TTTGCAAATACAACCCTTCAGA	GCAGAAGATACTGTACCACC
	Cdh5 (VEcad)	CACTGCTTTGGGAGCCTTC	GGGGCAGCGATTCATTTTCT
	Cldn5 (Claudin 5)	GCAAGGTGTATGAATCTGTGCT	GTCAAGGTAACAAAGAGTGCCA
Smooth muscle differentiation	Tagln (Sm22a)	CAACAAGGGTCCATCTACGG	ATCTGGGGGGCTACATCA
	Acta2 (a-SMA)	GTCCAGACATCAGGGAGTAA	TCGGATACTCAGCGTCAGGA
	Cnn1 (Calponin 1)	TCTGCACATTTAAACCGAGGTC	GCCAGTTGTTCTTACTTACGC
	Myh11 (smMHC)	AAGCTGCGGCTAGAGGTCA	CCCTCCCTTGTATGGCTGAG

Online Table 2. MS identified CTRP-9 binding membrane proteins

Gene names	Protein names	Mol. Weight (KDa)
Cdh2	N-cadherin	93.856
Tmc6	Transmembrane channel-like protein	12.582
Tmem143	Transmembrane protein 143	51.579
Tmem201	Transmembrane protein 201	25.66
Aoc3	Membrane primary amine oxidase	69.526
Vat1	Synaptic vesicle membrane protein VAT-1 homolog	42.521
Apmap	Adipocyte plasma membrane-associated protein	46.434
Smap2	Stromal membrane-associated protein 2	13.593

Supplemental Figures and Figure Legends



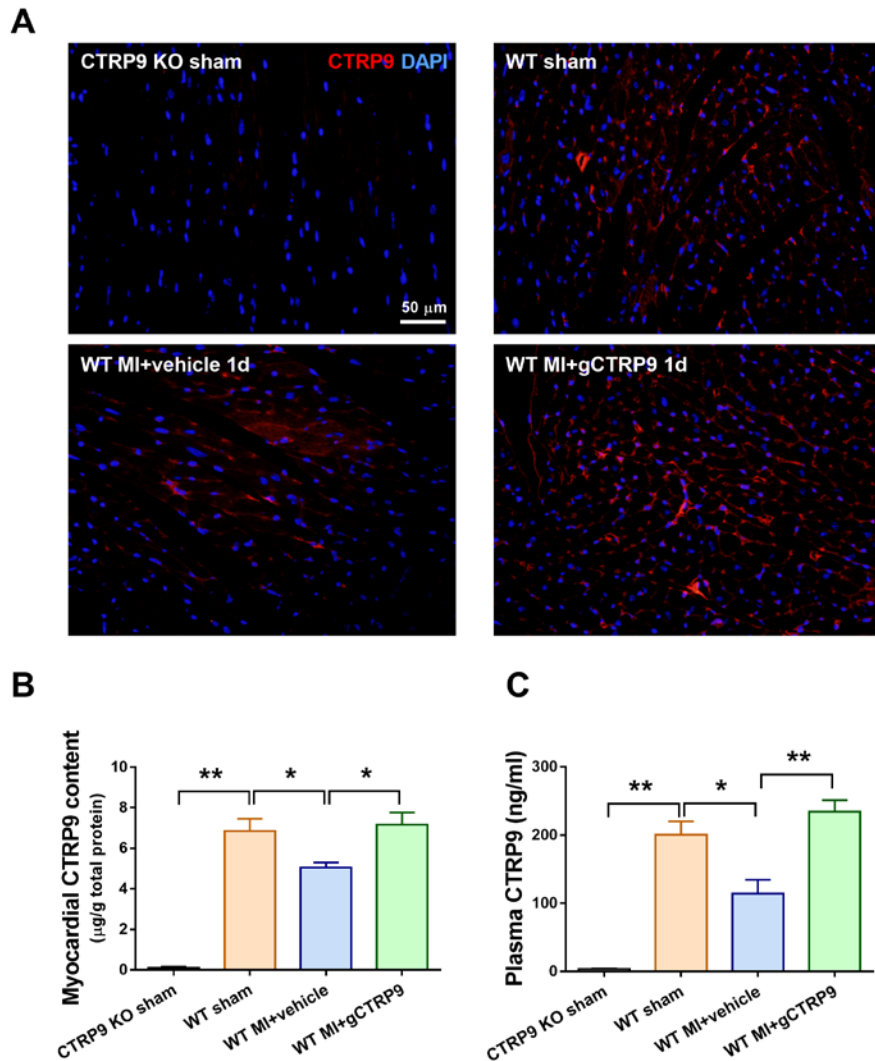
Supplemental Figure 1. Characterization of ADSCs.

A. ADSCs were isolated from EGFP-TG mice.

B-C. Flow cytometric analysis demonstrates ADSCs were positive for CD90.2 and CD105, and negative for CD45 and CD31. Data are mean \pm SEM. n=4.

D. Lipogenic and osteogenic differentiation of ADSCs were determined by histochemical staining of adipocytes (oil red O, middle panel) and osteocytes (Alizarin-Red, right panel).

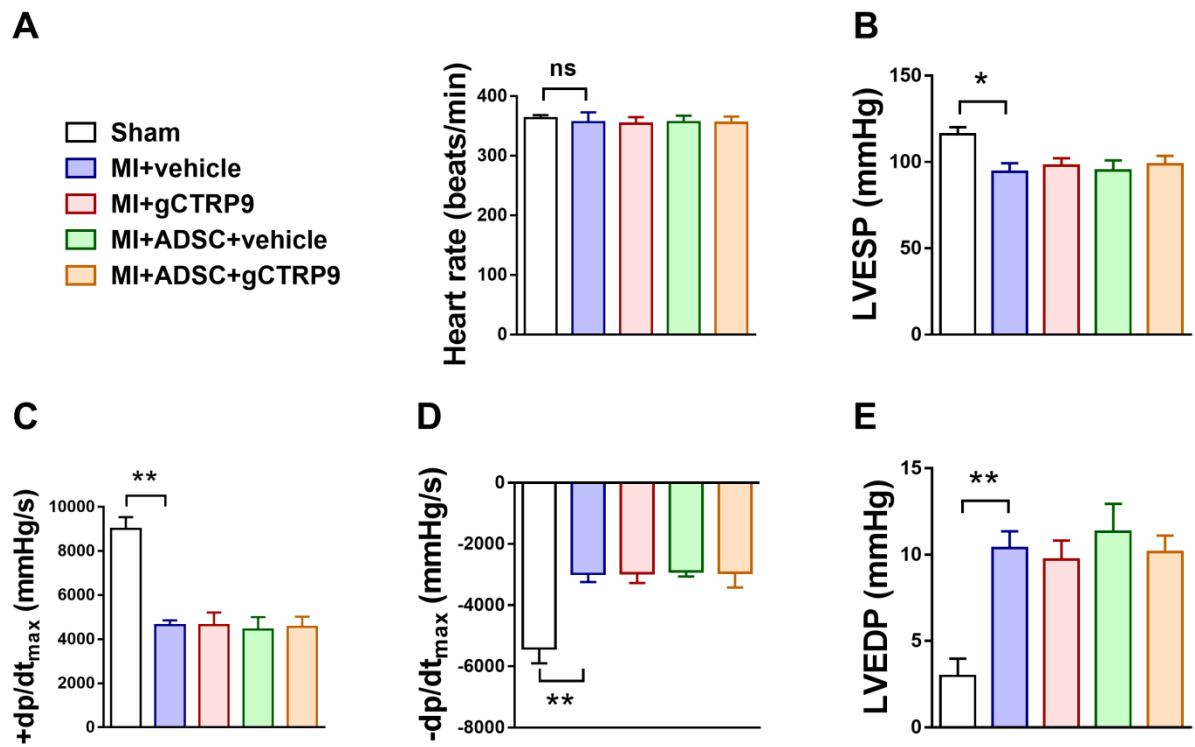
Abbreviations: ADSCs, adipose-derived mesenchymal stem cells.



Supplemental Figure 2. Intracardiac and plasma CTRP9 was downregulated by MI, but was restored by gCTR9 treatment.

A. Immunofluorescent staining of intracardiac CTRP9 in CTRP9 KO sham (upper left), WT sham (upper right), and 1 day post-MI WT heart with vehicle (lower left) or CTRP9 treatment (lower right).

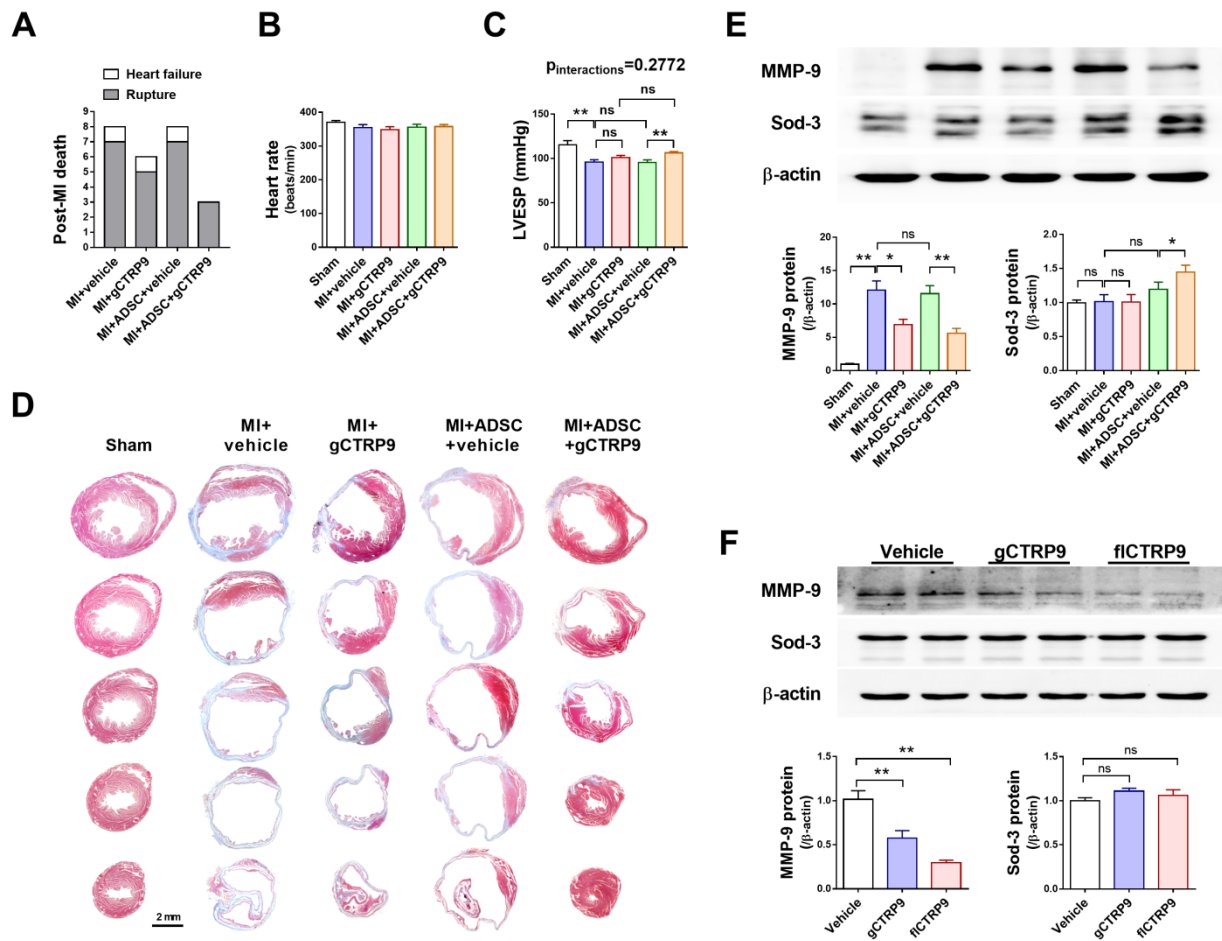
B-C. Myocardial CTRP9 content (B) and plasma CTRP9 (C) were downregulated by MI, and were restored by gCTR9. n=4-8. Data are mean ± SEM. *P<0.05, **P<0.01. Statistical significance was determined with one-way ANOVA followed by Bonferroni post-hoc test. *Abbreviations* : CTRP9 KO, CTRP9 knock-out.



Supplemental Figure 3. Initial cardiac dysfunction 12 hours after sham or MI.

Hemodynamic analyses including heart rate (A), left ventricular end-systolic pressure (LVESP) (B), +dp/dt_{max} (C), -dp/dt_{max} (D), and LV end diastolic pressure (LVEDP) (E) 12 hours after MI. n=5.

Data are mean ± SEM. *P<0.05, **P<0.01. NS, not significant. Statistical significance was determined by one-way ANOVA followed by Bonferroni post-hoc test.



Supplemental Figure 4.

A. Number of total deaths and death from left ventricular rupture in MI groups (15 mice per group).

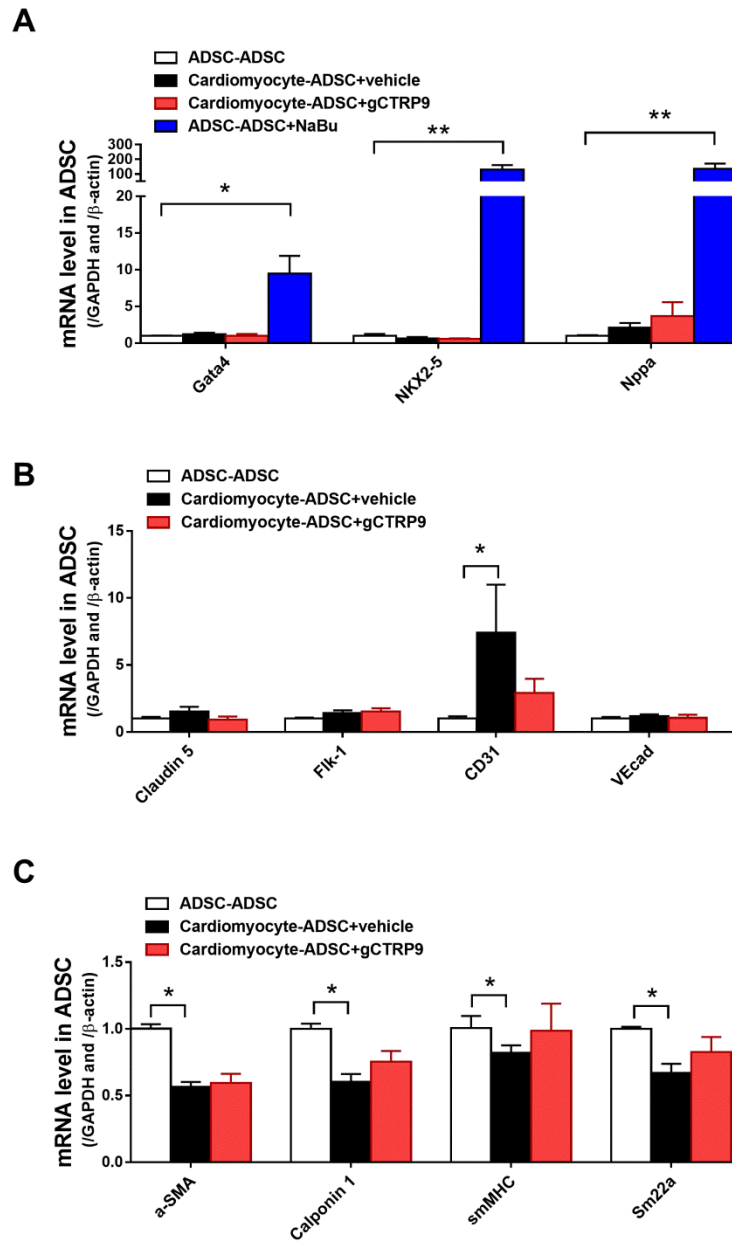
B and C. Hemodynamic analyses including heart rate (B) and left ventricular end-systolic pressure (LVESP, C) 4 weeks after MI. n=10-19.

D. The five sections of the representative Masson's trichrome staining 4 weeks after MI.

E. Western blots and quantification protein expression of MMP-9 and Sod-3 in infarct border zone 1 day after MI. n=4.

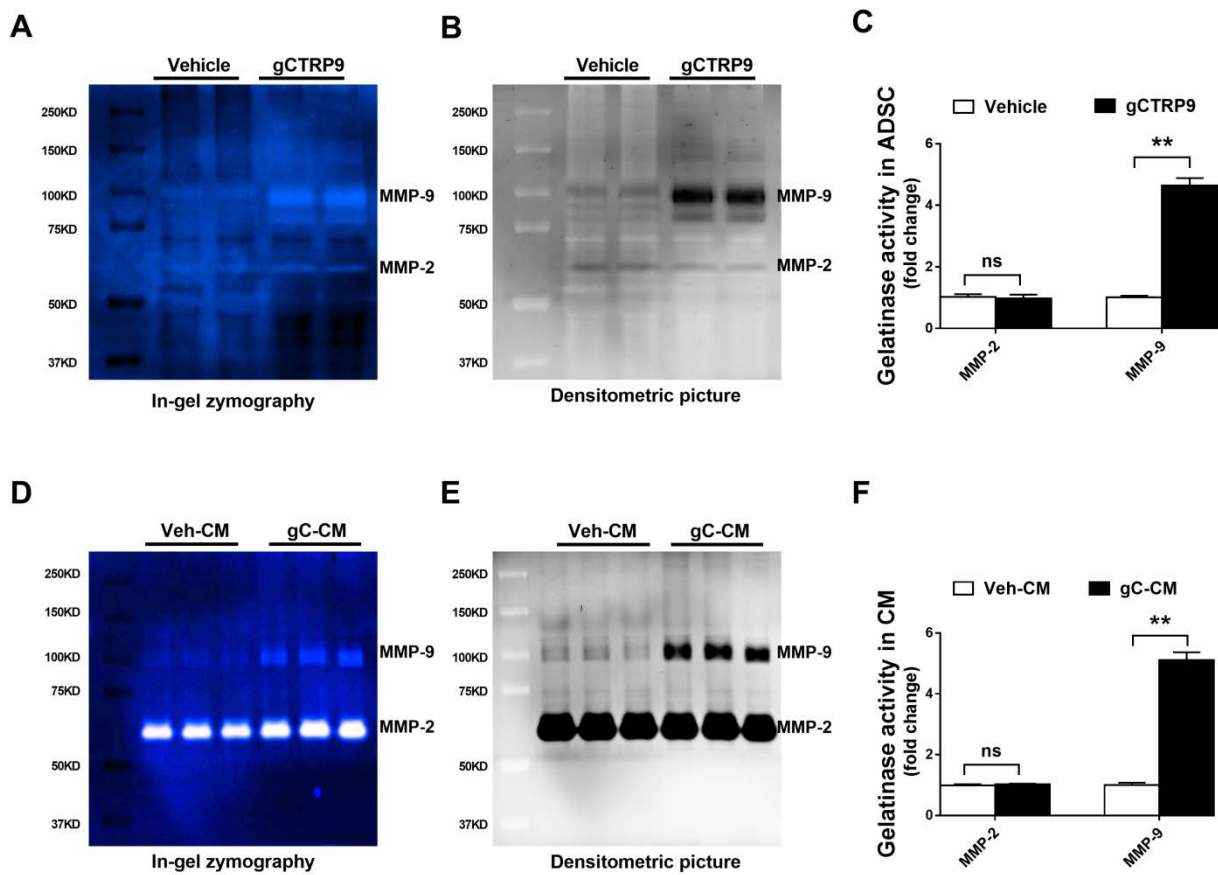
F. Western blots and quantification protein expression of MMP-9 and Sod-3 in neonatal mouse ventricular cardiomyocytes. gCTRP9 dose 2μg/mL, fICTRP9 dose 5μg/mL, 24 hours. n=4.

Data are mean ± SEM. *P<0.05, **P<0.01. NS, not significant. Post-MI deaths were analyzed by Chi-square test. Heart rate and LVESP were analyzed by two-way ANOVA followed by Bonferroni post-hoc test. Other data were analyzed with one-way ANOVA followed by Bonferroni post-hoc test.



Supplemental Figure 5. CTRP9 did not affect cardiogenic, vasculogenic, or fibrogenic differentiation of ADSCs after 7 days of co-culture with neonatal mouse ventricular cardiomyocytes.

A-C. Real time PCR analysis of cardiogenic (A), vasculogenic (B), and fibrogenic (C) gene expression in ADSCs co-cultured with ADSCs or cardiomyocytes for 7 days. gCTRP9 dose 2µg/mL, 7 days. n=4-8. Data are mean ± SEM. *P<0.05, **P<0.01. Statistical significance was determined with one-way ANOVA followed by Bonferroni post-hoc test. NaBu was used as a positive control for inducing cardiogenic of mesenchymal stem cells. *Abbreviations:* NaBu, sodium butyrate (5mM, 7 days).

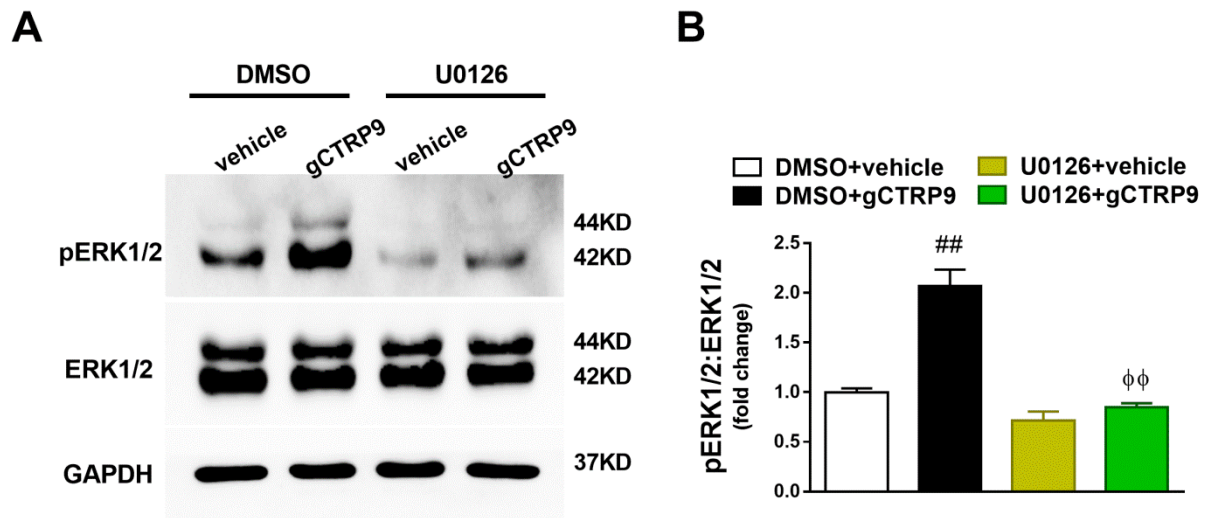


Supplemental Figure 6. In-gel zymography assay of getatinases (MMP-2 and MMP-9) in protein samples and conditioned medium of ADSCs.

A-C. Original in-gel zymography picture (A), densitometric picture (B), and quantification of MMP-2 and MMP-9 activity (C) in protein samples of ADSCs.

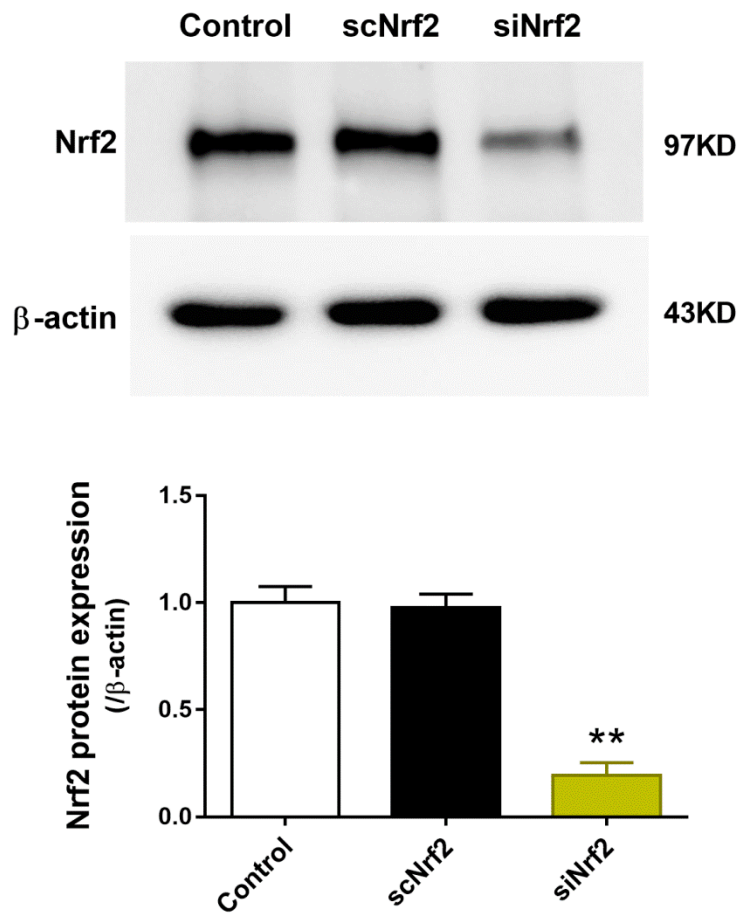
D-F. Original in-gel zymography picture (D), densitometric picture (E), and quantification of MMP-2 and MMP-9 activity (F) in conditioned medium (CM) of ADSCs.

Data are mean \pm SEM. n=4-5. **P<0.01. NS, not significant. Statistical significance was determined with unpaired student's t test. *Abbreviations:* veh-CM, conditioned medium collected from vehicle treated ADSCs; gC-CM, conditioned medium collected from gCTRP9 (2 μ g/mL, 24 hours)-treated ADSCs.



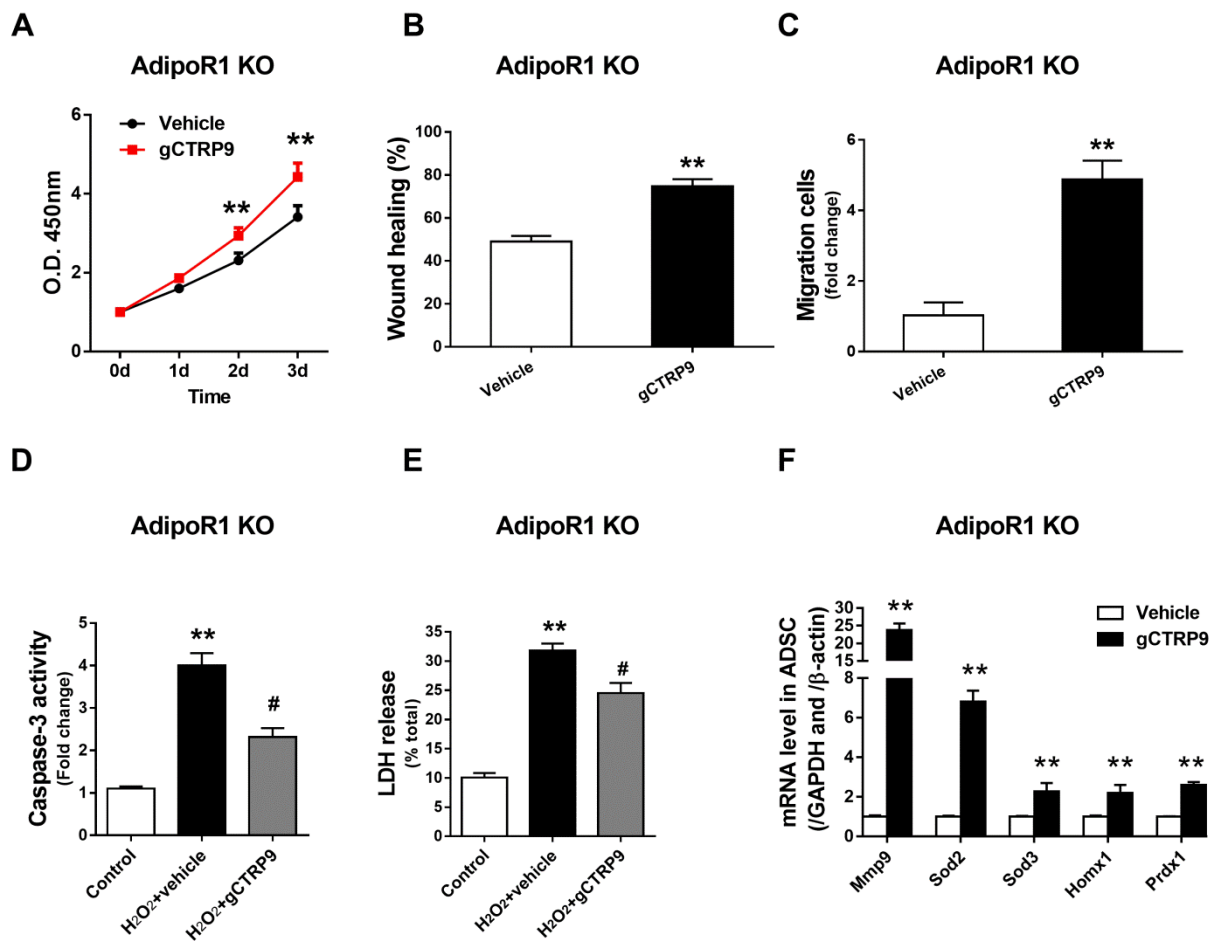
Supplemental Figure 7. U0126, an ERK1/2 activation inhibitor, significantly blocked ERK1/2 phosphorylation by gCTRP9 in ADSCs.

(A) Western blots, (B) quantification. gCTRP9: 2 μ g/mL, 15 minutes. U0126: 10 μ M, 2 hours before gCTRP9 treatment. n=4. ##P<0.01 vs. DMSO+vehicle; $\phi\phi$ P<0.01 vs. DMSO+gCTRP9. Statistical significance was determined with one-way ANOVA followed by Bonferroni post-hoc test.



Supplemental Figure 8. Nrf2 siRNA decreased Nrf2 protein expression in ADSCs.

Western blots and quantification of Nrf2 in ADSCs cell lysis 72 hours after transfection. n=3. Data are mean \pm SEM. **P<0.01 vs. scNrf2. Statistical significance was determined with one-way ANOVA followed by Bonferroni post-hoc test. *Abbreviations:* scNrf2, Nrf2 scramble RNA (100nM); siNrf2, Nrf2 siRNA (100nM).



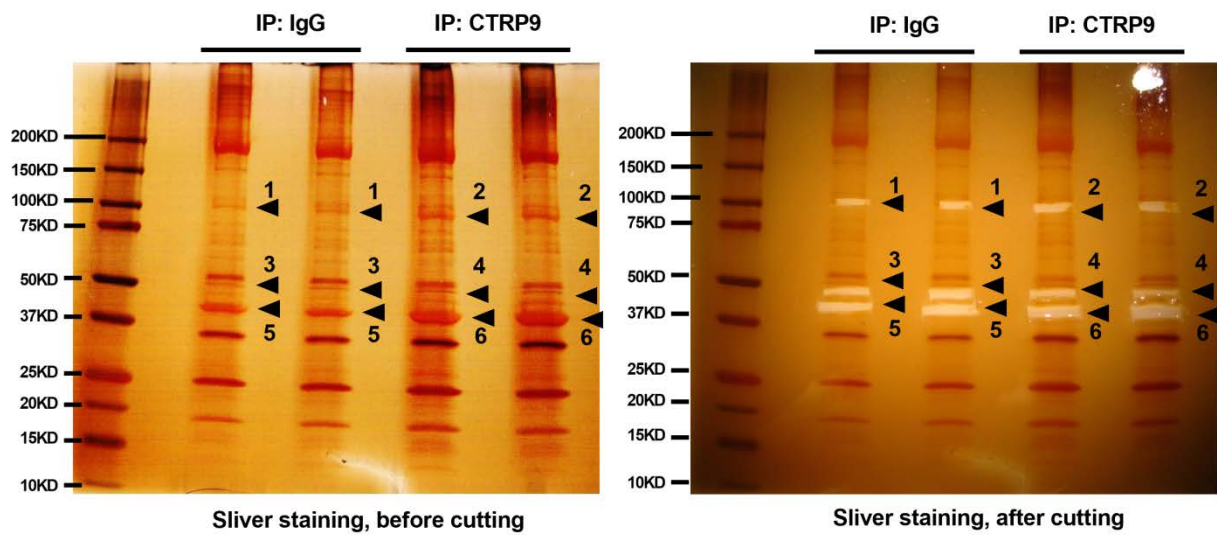
Supplemental Figure 9. CTRP9 promoted ADSCs proliferation and survival in an adiponectin receptor 1 (AdipoR1)-independent manner.

A. ADSCs proliferation curves over 3 day period. n=6-9. gCTRP9: 2μg/mL. **P<0.01 vs. Vehicle. Statistical significance was determined with two-way ANOVA followed by Bonferroni post-hoc test.

B-C. Wound healing assay (B) and Matrigel pre-coated transwell assay (C) were performed 24 hours after gCTRP9 (2μg/mL) or vehicle treatment. n=4. **P<0.01 vs. Vehicle. Statistical significance was determined with unpaired student's t test.

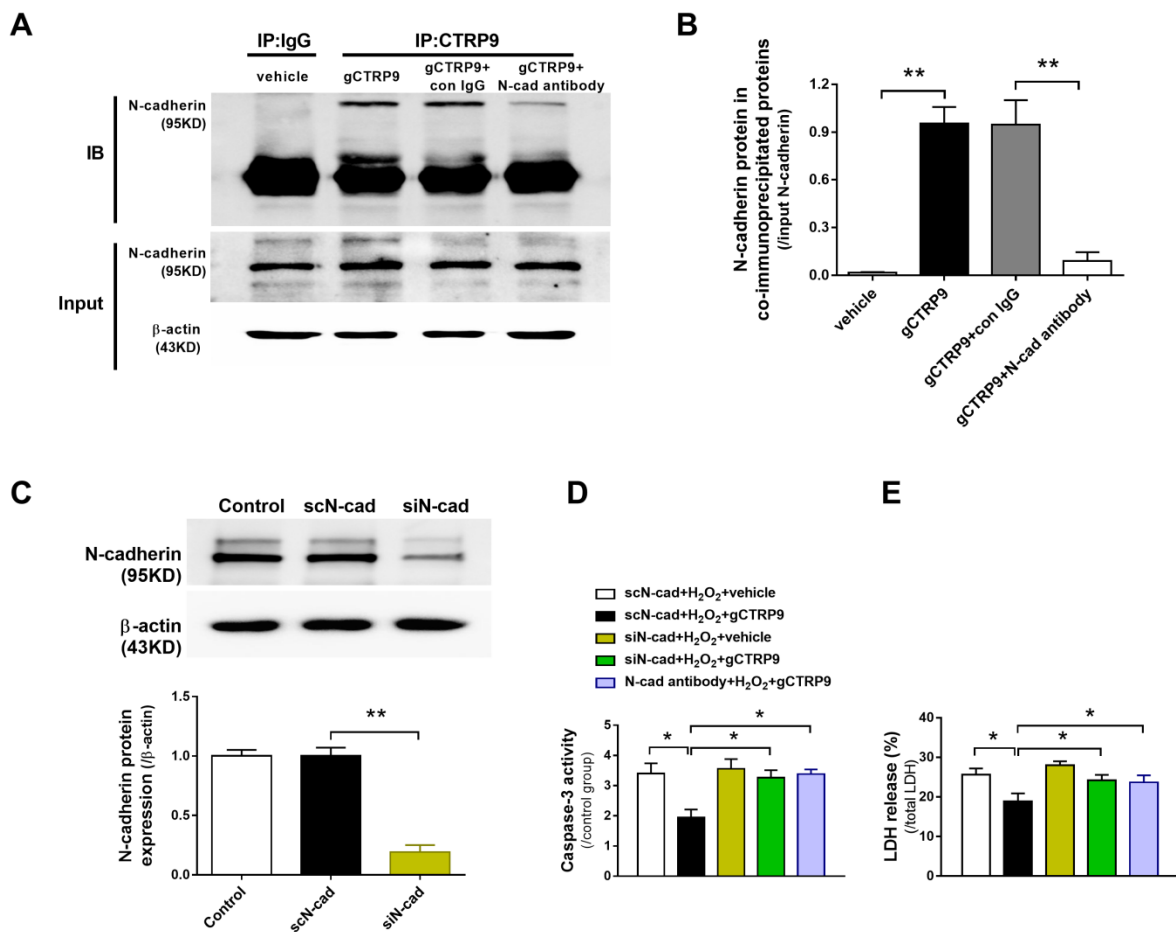
D-E. ADSCs apoptosis and death were determined by caspase-3 activity (D, n=6) and LDH release (E, n=10). gCTRP9: 2μg/mL, 24h. H₂O₂: 200μM, 6h. **P<0.01 vs. Control; #P<0.05 vs. H₂O₂+vehicle. Statistical significance was determined with one-way ANOVA followed by Bonferroni post-hoc test.

F. mRNA expression of Mmp9, Sod2, Sod3, Homx1, and Prdx1 in ADSCs treated with 2μg/mL gCTRP9 or vehicle for 24 hours. n=4-8. Data are mean ± SEM. **P<0.01 vs. Vehicle. Statistical significance was determined with unpaired student's t test.



Supplemental Figure 10. Silver staining of CTRP9 and control IgG co-immunoprecipitated proteins in gel.

Cardiac tissue proteins were co-immunoprecipitated by rabbit anti-CTRP9 antibody or rabbit IgG overnight. The co-immunoprecipitated proteins were separated by electrophoresis, and silver stained (left). The differential regions were cut (right) for further analysis.



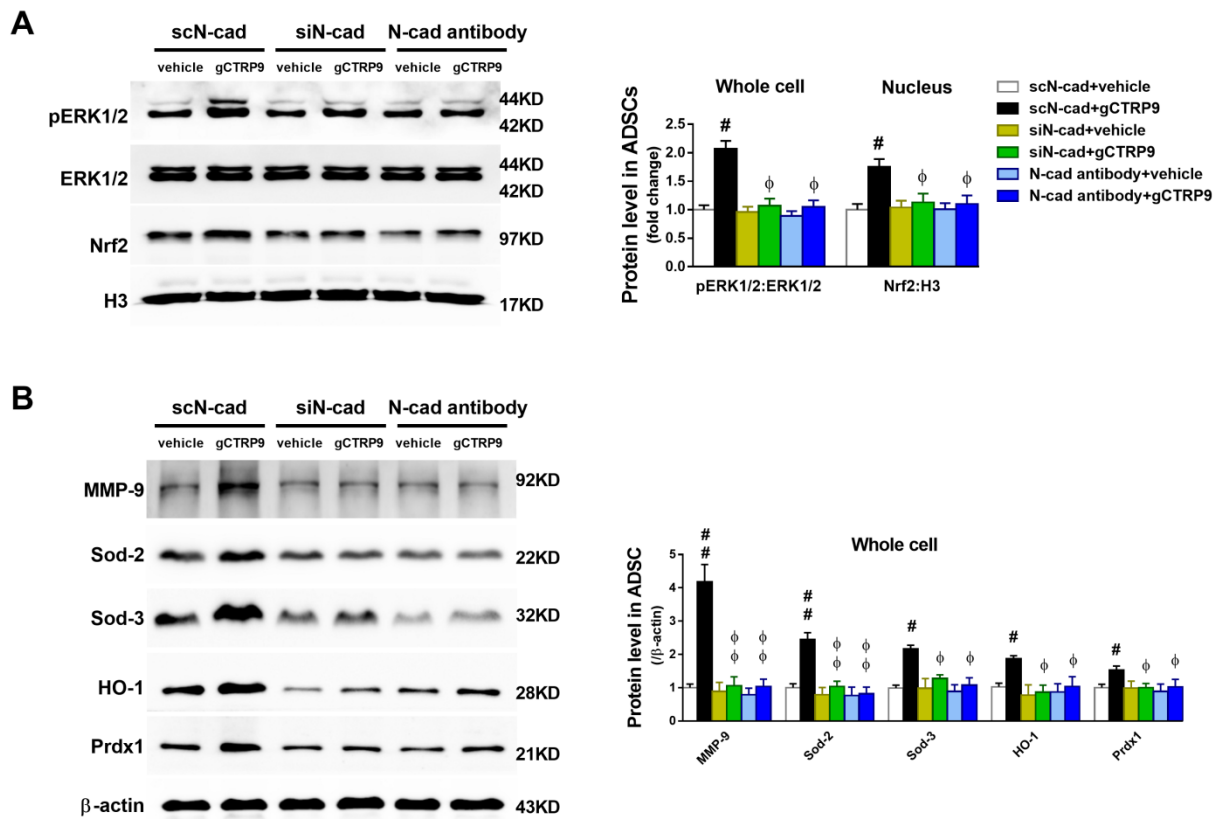
Supplemental Figure 11.

A-B. N-cadherin blocking antibody inhibited CTRP9/N-cadherin interaction in ADSCs. **A.** Co-immunoprecipitation (Co-IP) and immunoblot (IB) analysis of N-cadherin with gCTR9 in ADSCs. ADSCs were treated with vehicle, gCTR9, N-cadherin blocking antibody (N-cad antibody) plus gCTR9 or control IgG (con IgG) plus gCTR9. **B.** Quantification of N-cadherin in co-immunoprecipitated proteins. n=3.

C. N-cadherin siRNA decreased N-cadherin protein expression in ADSCs. Western blots and quantification of N-cadherin in ADSCs cell lysis 72 hours after transfection. n=3.

D-E. CTRP9 protected ADSCs from H₂O₂ induced injury via N-cadherin. **D.** ADSCs apoptosis, determined by caspase-3 activity (n=4). **E.** ADSCs death, determined by LDH release (n=8). gCTR9: 2.0 μ g/ml, 24 hours. H₂O₂: 200 μ M, 6 hours.

Data are mean \pm SEM. *P<0.05, **P<0.01. Statistical significance was determined with one-way ANOVA followed by Bonferroni post-hoc test. *Abbreviations:* scN-cad, N-cadherin scramble RNA (100nM); siN-cad, N-cadherin siRNA (100nM); con IgG, control IgG (5 μ g/mL); N-cad antibody, N-cadherin blocking antibody (5 μ g/mL, 2 hours prior to gCTR9 administration).

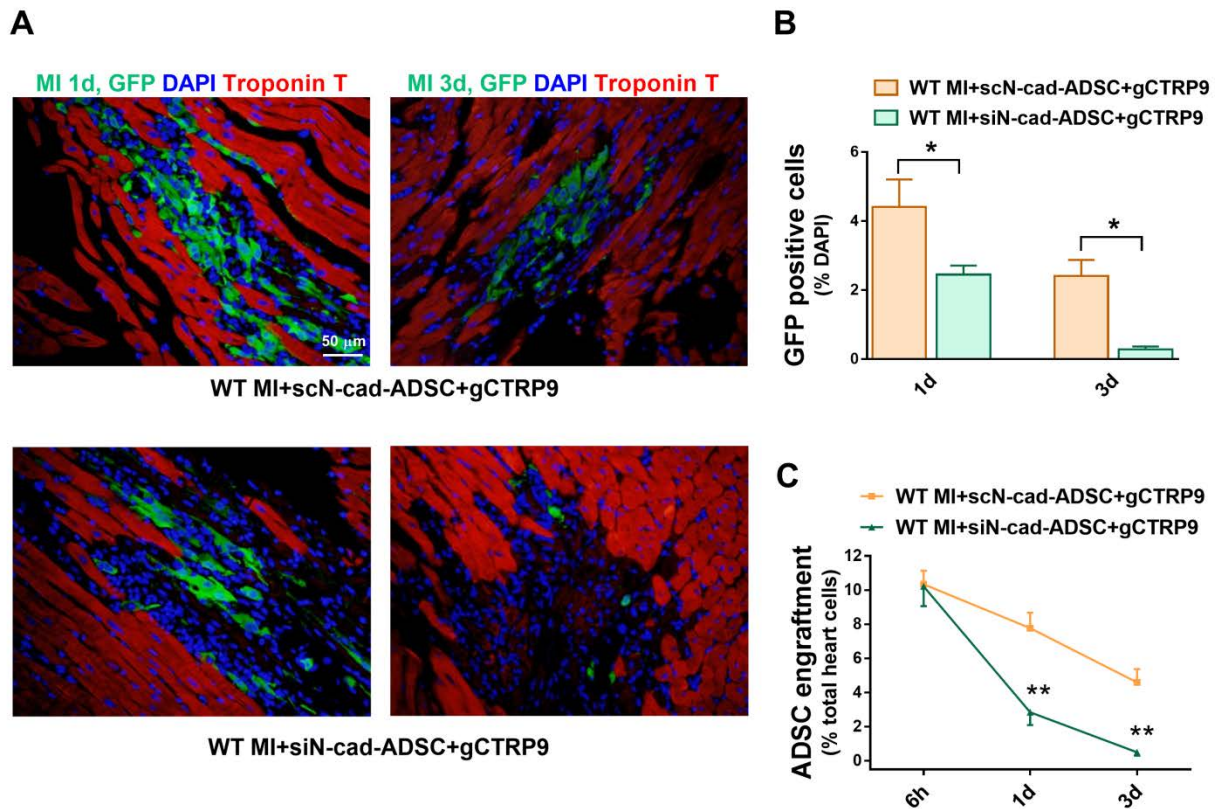


Supplemental Figure 12. CTRP9 promoted ERK1/2 activation and its downstream molecule via N-cadherin.

A. Western blots (left) and quantification (right) of phospho-ERK1/2, total ERK1/2, nuclear Nrf2, and H3 in ADSCs.

B. Western blots (left) and quantification (right) of MMP-9, Sod-2, Sod-3, HO-1, and Prdx1 in ADSCs cell lysis.

Data are mean \pm SEM. $n=4-6$. $^{\#}P<0.05$, $^{\#\#}P<0.01$ vs. scN-cad+vehicle; $^{\Phi}P<0.05$, $^{\Phi\Phi}P<0.01$ vs. scN-cad+gCTRP9. Statistical significance was determined with one-way ANOVA followed by Bonferroni post-hoc test. *Abbreviations:* scN-cad, N-cadherin scramble RNA; siN-cad, N-cadherin siRNA; N-cadherin antibody: N-cadherin blocking antibody (5 μ g/mL), 2 hours before gCTRP9 (2 μ g/mL, 24 hours) treatment.



Supplemental Figure 13. N-cadherin knock-down decreased ADSCs survival in peri-infarct area 1 and 3 days after MI in the presence of gCTRP9.

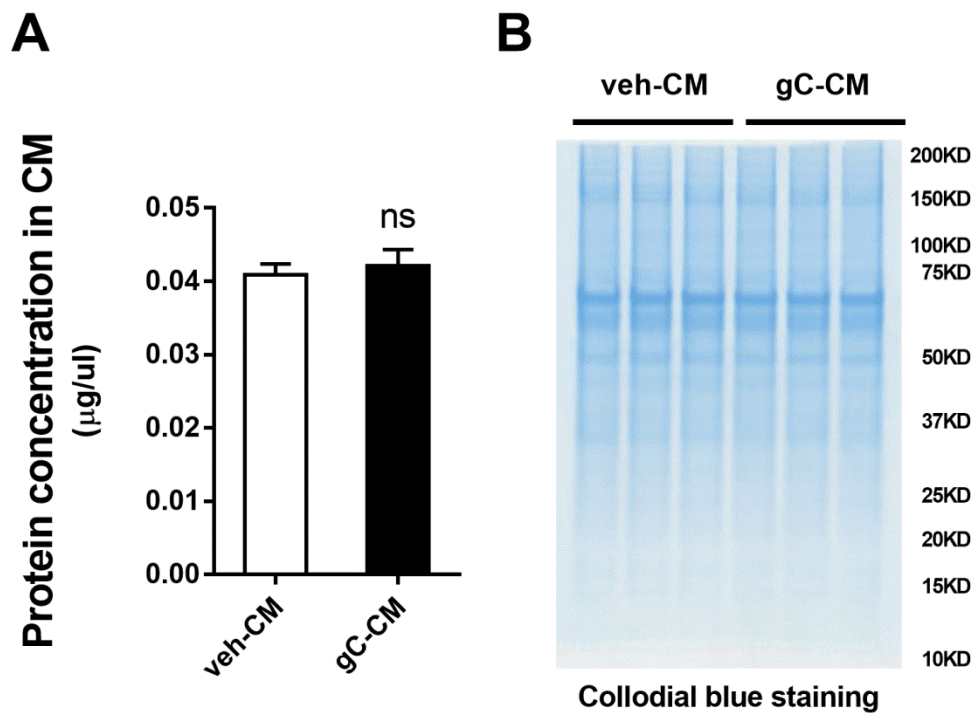
A. Representative images of EGFP-ADSCs in hearts 1 and 3 days after MI. Heart tissue was immunostained for GFP (green), DAPI (blue), and Troponin T (red).

B. Quantification of EGFP-ADSCs in the peri-infarct area was determined by the number of GFP-positive cells per total nuclei. n=20 from 4 mice.

C. ADSCs engraftment was quantified as the number of GFP-positive cells per 100 heart cells in apex region. n=4 mice.

Data are mean \pm SEM. *P<0.05. **P<0.01 vs. WT MI+scN-cad-ADSC+gCTRP9. Statistical significance was determined with two-way ANOVA followed by Bonferroni post-hoc test.

Abbreviations: scN-cad, N-cadherin scramble RNA; siN-cad, N-cadherin siRNA.

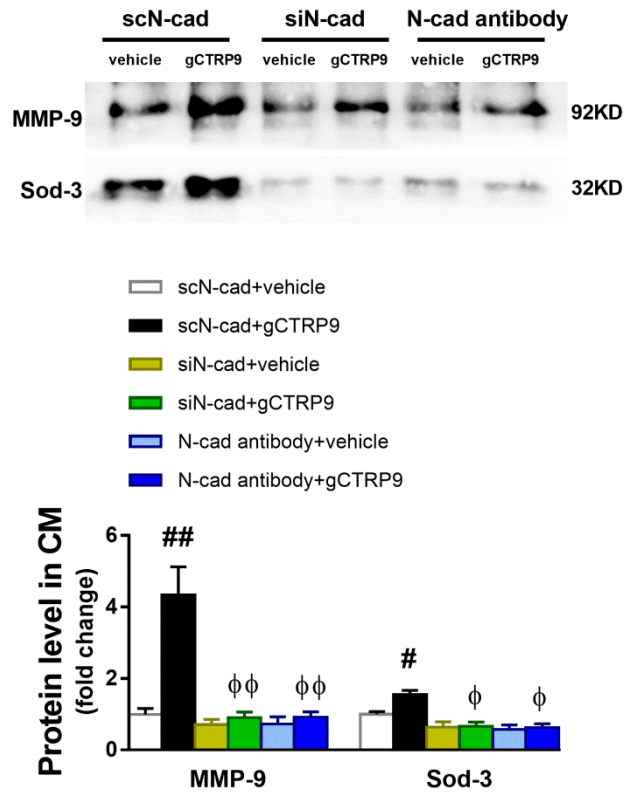


Supplemental Figure 14. CTRP9 did not affect total protein concentration in conditioned medium (CM) of ADSCs.

A. Total protein concentration in CM measured by Bio-Rad Protein Assay. n=10. Data are mean \pm SEM. Data was analyzed with unpaired student's t test. *Abbreviations:* NS, not significant.

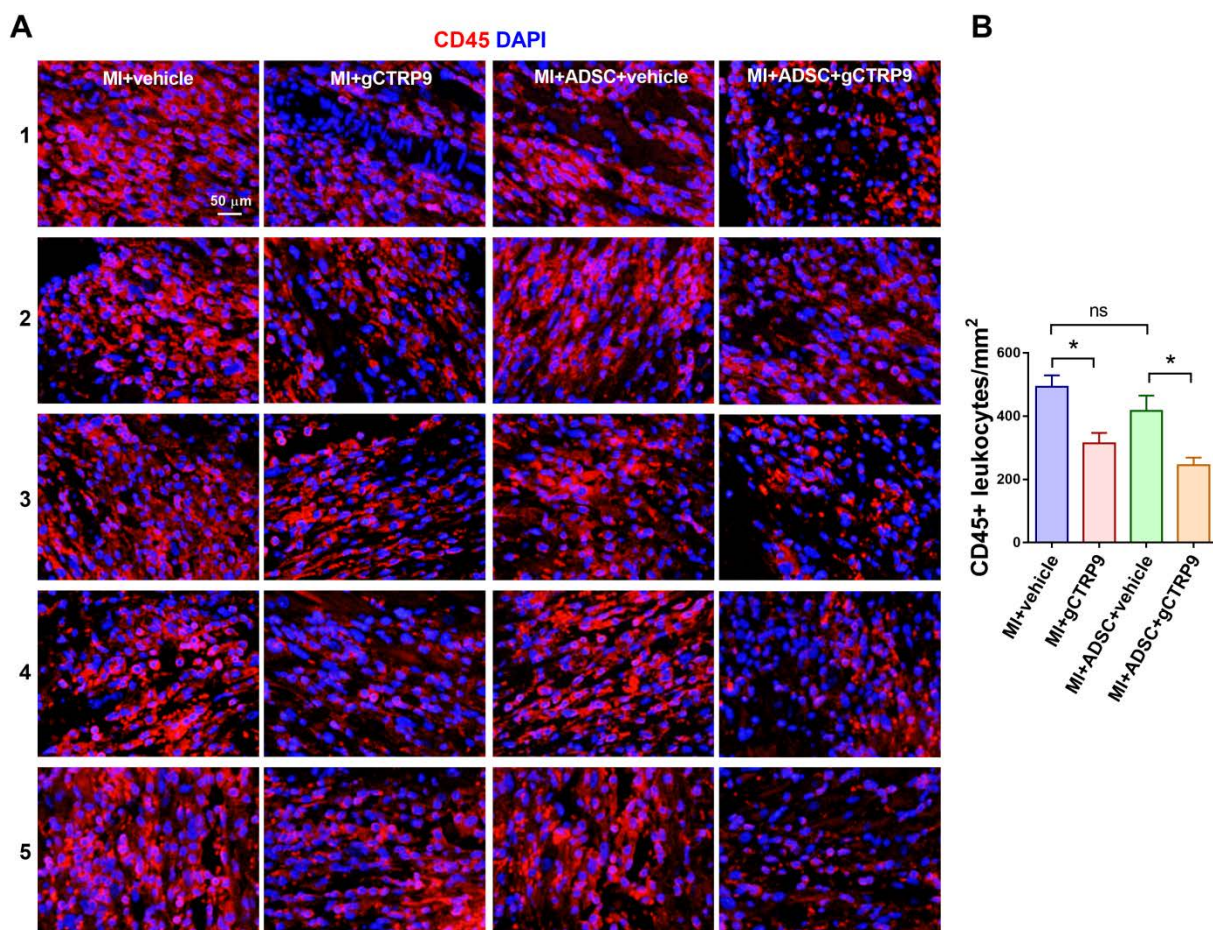
B. Colloidal blue staining gel, demonstrating equal amounts of protein between two groups. n=3.

Abbreviations: veh-CM, conditioned medium collected from vehicle treated ADSCs; gC-CM, conditioned medium collected from gCTRP9 (2µg/mL, 24 hours)-treated ADSCs.



Supplemental Figure 15. CTRP9 induced extracellular secretion of MMP-9 and Sod-3 via N-cadherin in ADSCs.

Western blots (upper) and quantification (lower) of MMP-9 and Sod-3 in conditioned medium (CM) of ADSCs. Data are mean \pm SEM. n=4. #P<0.05, ##P<0.01 vs. scN-cad+vehicle; Φ P<0.05, $\Phi\Phi$ P<0.01 vs. scN-cad+gCTRP9. Statistical significance was determined with one-way ANOVA followed by Bonferroni post-hoc test. *Abbreviations:* scN-cad, N-cadherin scramble RNA; siN-cad, N-cadherin siRNA; N-cadherin antibody: N-cadherin blocking antibody (5 μ g/mL), 2 hours before gCTRP9 (2 μ g/mL, 24 hours) treatment.



Supplemental Figure 16. CD45 (red) and DAPI (blue) immunostaining in infarct border zone 7 days after MI. n=5.

Data are mean ± SEM. *P<0.05. NS, not significant. Data were analyzed with one-way ANOVA followed by Bonferroni post-hoc test.

Supplemental References

1. Okabe M, Ikawa M, Kominami K, Nakanishi T and Nishimune Y. 'Green mice' as a source of ubiquitous green cells. *FEBS Lett.* 1997;407:313-319.
2. Wei Z, Lei X, Petersen PS, Aja S and Wong GW. Targeted deletion of C1q/TNF-related protein 9 increases food intake, decreases insulin sensitivity, and promotes hepatic steatosis in mice. *Am J Physiol Endocrinol Metab.* 2014;306:E779-790.
3. Takahashi M, Suzuki E, Oba S, Nishimatsu H, Kimura K, Nagano T, Nagai R and Hirata Y. Adipose tissue-derived stem cells inhibit neointimal formation in a paracrine fashion in rat femoral artery. *Am J Physiol Heart Circ Physiol.* 2010;298:H415-423.
4. Bai X, Yan Y, Song YH, Seidensticker M, Rabinovich B, Metzler R, Bankson JA, Vykoukal D and Alt E. Both cultured and freshly isolated adipose tissue-derived stem cells enhance cardiac function after acute myocardial infarction. *Eur Heart J.* 2010;31:489-501.
5. Gao E, Lei YH, Shang X, Huang ZM, Zuo L, Boucher M, Fan Q, Chuprun JK, Ma XL and Koch WJ. A novel and efficient model of coronary artery ligation and myocardial infarction in the mouse. *Circ Res.* 2010;107:1445-1453.
6. Zhang F, Xia Y, Yan W, Zhang H, Zhou F, Zhao S, Wang W, Zhu D, Xin C, Lee Y, Zhang L, He Y, Gao E and Tao L. Sphingosine 1-phosphate signaling contributes to cardiac inflammation, dysfunction, and remodeling following myocardial infarction. *Am J Physiol Heart Circ Physiol.* 2016;310:H250-261.
7. Wang WE, Yang D, Li L, Wang W, Peng Y, Chen C, Chen P, Xia X, Wang H, Jiang J, Liao Q, Li Y, Xie G, Huang H, Guo Y, Ye L, Duan DD, Chen X, Houser SR and Zeng C. Prolyl hydroxylase domain protein 2 silencing enhances the survival and paracrine function of transplanted adipose-derived stem cells in infarcted myocardium. *Circ Res.* 2013;113:288-300.
8. Choi YS, Dusing GJ, Stubbs S, Arunothayaraj S, Han XL, Collas P, Morrison WA and Dilley RJ. Differentiation of human adipose-derived stem cells into beating cardiomyocytes. *J Cell Mol Med.* 2010;14:878-889.
9. Moore JBt, Zhao J, Keith MC, Amraotkar AR, Wysoczynski M, Hong KU and Bolli R. The Epigenetic Regulator HDAC1 Modulates Transcription of a Core Cardiogenic Program in Human Cardiac Mesenchymal Stromal Cells Through a p53-Dependent Mechanism. *Stem Cells.* 2016;34:2916-2929.
10. Wang Y, Wang X, Lau WB, Yuan Y, Booth D, Li JJ, Scalia R, Preston K, Gao E, Koch W and Ma XL. Adiponectin inhibits tumor necrosis factor-alpha-induced vascular inflammatory response via caveolin-mediated ceramidase recruitment and activation. *Circ Res.* 2014;114:792-805.
11. Hinkel R, Lange P, Petersen B, Gottlieb E, Ng JK, Finger S, Horstkotte J, Lee S, Thormann M, Knorr M, El-Aouni C, Boekstegers P, Reichart B, Wenzel P, Niemann H and Kupatt C. Heme Oxygenase-1 Gene Therapy Provides Cardioprotection Via Control of Post-Ischemic Inflammation: An Experimental Study in a Pre-Clinical Pig Model. *J Am Coll Cardiol.* 2015;66:154-165.
12. Fuijkschoot WW, Groothuizen WE, Appelman Y, Radonic T, van Royen N, van Leeuwen MA, Krijnen PA, van der Wal AC, Smulders YM and Niessen HW. Inflammatory cell content of coronary thrombi is dependent on thrombus age in patients with ST-elevation myocardial infarction. *J Cardiol.* 2017;69:394-400.
13. Yan X, Anzai A, Katsumata Y, Matsushashi T, Ito K, Endo J, Yamamoto T, Takeshima A, Shinmura K, Shen W, Fukuda K and Sano M. Temporal dynamics of cardiac immune cell accumulation following acute myocardial infarction. *J Mol Cell Cardiol.* 2013;62:24-35.
14. Wu SP, Kao CY, Wang L, Creighton CJ, Yang J, Donti TR, Harmancey R, Vasquez HG, Graham

- BH, Bellen HJ, Taegtmeyer H, Chang CP, Tsai MJ and Tsai SY. Increased COUP-TFII expression in adult hearts induces mitochondrial dysfunction resulting in heart failure. *Nat Commun*. 2015;6:8245.
15. Ashrafian H, Czibik G, Bellahcene M, Aksentijevic D, Smith AC, Mitchell SJ, Dodd MS, Kirwan J, Byrne JJ, Ludwig C, Isackson H, Yavari A, Stottrup NB, Contractor H, Cahill TJ, Sahgal N, Ball DR, Birkler RI, Hargreaves I, Tennant DA, Land J, Lygate CA, Johannsen M, Kharbanda RK, Neubauer S, Redwood C, de Cabo R, Ahmet I, Talan M, Gunther UL, Robinson AJ, Viant MR, Pollard PJ, Tyler DJ and Watkins H. Fumarate is cardioprotective via activation of the Nrf2 antioxidant pathway. *Cell Metab*. 2012;15:361-371.
 16. Ikonomidis JS, Barbour JR, Amani Z, Stroud RE, Herron AR, McClister DM, Jr., Camens SE, Lindsey ML, Mukherjee R and Spinale FG. Effects of deletion of the matrix metalloproteinase 9 gene on development of murine thoracic aortic aneurysms. *Circulation*. 2005;112:242-248.
 17. Su H, Yuan Y, Wang XM, Lau WB, Wang Y, Wang X, Gao E, Koch WJ and Ma XL. Inhibition of CTRP9, a novel and cardiac-abundantly expressed cell survival molecule, by TNF α -initiated oxidative signaling contributes to exacerbated cardiac injury in diabetic mice. *Basic Res Cardiol*. 2013;108:315.
 18. Teng L, Bennett E and Cai C. Preconditioning c-Kit-positive Human Cardiac Stem Cells with a Nitric Oxide Donor Enhances Cell Survival through Activation of Survival Signaling Pathways. *J Biol Chem*. 2016;291:9733-9747.
 19. Wong GW, Krawczyk SA, Kitidis-Mitrokostas C, Ge G, Spooner E, Hug C, Gimeno R and Lodish HF. Identification and characterization of CTRP9, a novel secreted glycoprotein, from adipose tissue that reduces serum glucose in mice and forms heterotrimers with adiponectin. *Faseb j*. 2009;23:241-258.
 20. Wei CJ, Francis R, Xu X and Lo CW. Connexin43 associated with an N-cadherin-containing multiprotein complex is required for gap junction formation in NIH3T3 cells. *J Biol Chem*. 2005;280:19925-19936.
 21. Arnott D, O'Connell KL, King KL and Stults JT. An integrated approach to proteome analysis: identification of proteins associated with cardiac hypertrophy. *Anal Biochem*. 1998;258:1-18.
 22. Hu X, Xu Y, Zhong Z, Wu Y, Zhao J, Wang Y, Cheng H, Kong M, Zhang F, Chen Q, Sun J, Li Q, Jin J, Li Q, Chen L, Wang C, Zhan H, Fan Y, Yang Q, Yu L, Wu R, Liang J, Zhu J, Wang Y, Jin Y, Lin Y, Yang F, Jia L, Zhu W, Chen J, Yu H, Zhang J and Wang J. A Large-Scale Investigation of Hypoxia-Preconditioned Allogeneic Mesenchymal Stem Cells for Myocardial Repair in Nonhuman Primates: Paracrine Activity Without Remuscularization. *Circ Res*. 2016;118:970-983.
 23. Xue J, Li X, Lu Y, Gan L, Zhou L, Wang Y, Lan J, Liu S, Sun L, Jia L, Mo X and Li J. Gene-modified mesenchymal stem cells protect against radiation-induced lung injury. *Mol Ther*. 2013;21:456-465.